Letters in Applied NanoBioScience
Open-Access Journal (ISSN: 2284-6808)

Article
Volume 15, Issue 3, 2026, 87
https://doi.org/10.33263/LIANBS153.087

Discovery of Catechin from *Acacia arabica* as a Potential Inhibitor of New Delhi Metallo-β-lactamase-1 (NDM-1): Insights from *In Silico* Docking and Antibacterial Assays

Ajay Kumar [1], Sapna Redhu [1], Ajmer Singh Grewal [2,*], Suresh Kumar Gahlawat [1,*]

[1] Department of Biotechnology, Chaudhary Devi Lal University, Sirsa, Haryana, India; ajaychahal21@gmail.com (A.K.); sapnabalhara1@gmail.com (S.R.); skgcdlu@gmail.com (S.K.G.);
[2] Guru Gobind Singh College of Pharmacy, Yamuna Nagar, Haryana, India; ajmergrewal2007@gmail.com;
* Correspondence: ajmergrewal2007@gmail.com (A.S.G.); skgcdlu@gmail.com (S.K.G.);

Received: 7.06.2025; Accepted: 20.02.2026; Published: 01.07.2026

Abstract: The global rise in antimicrobial resistance, particularly due to the proliferation of metallo-β-lactamase enzymes such as New Delhi metallo-β-lactamase-1 (NDM-1), presents a significant challenge in clinical therapeutics. This study explores the inhibitory potential of catechin derived from *Acacia arabica* against NDM-1 using integrated *in silico* and *in vitro* approaches. *In silico* docking studies were conducted using AutoDock Vina, wherein catechin demonstrated significant binding affinity with key active site residues and metal (Zn) cofactor of the NDM-1 protein. Pharmacokinetic and toxicity profiles of phytoconstituents were assessed using SwissADME and pkCSM tools to evaluate drug-likeness and safety. Among several screened compounds, catechin exhibited favorable ADMET properties and strong docking scores. The antibacterial activity of *A. arabica* extracts was evaluated against NDM-1-producing *Escherichia coli* strains using modified disk diffusion assays. Acetone extracts displayed the highest inhibitory zones, which further increased when administered alongside amoxicillin, indicating a potentiated effect. This study highlights the promising role of plant-derived catechins as lead compounds for the development of NDM-1 inhibitors and underscores the therapeutic potential of *A. arabica* in counteracting antimicrobial resistance. The findings support further investigation and structural optimization of catechin-based inhibitors targeting NDM-1.

Keywords: New Delhi metallo-β-lactamase-1; NDM-1 inhibitors; *Escherichia coli*; antimicrobial resistance; plant-derived inhibitors.

1. Introduction

Antimicrobial resistance (AMR) has emerged as a formidable threat to global health, characterized by the increasing ineffectiveness of conventional antibiotics against pathogenic microorganisms. The inappropriate and excessive use of antibiotics in clinical and agricultural settings has hastened the evolution of resistant bacterial strains, posing an urgent challenge to public health systems worldwide. Projections from the landmark UK Review on "*Antimicrobial Resistance*" estimate that AMR could account for up to 10 million deaths annually by 2050 if not addressed through coordinated international efforts [1,2]. Recognizing its magnitude, the World Health Organization (WHO) and other international bodies have

identified AMR as a priority issue demanding immediate and sustained action [3]. Among the Gram-negative bacteria contributing to this crisis, Escherichia coli occupies a prominent position due to its high prevalence and capacity to acquire resistance genes. Data from the 2022 Global Antimicrobial Resistance and Use Surveillance System (GLASS) report indicate that approximately 42% of *Escherichia coli* isolates are resistant to third-generation cephalosporins [4]. In India, surveillance data compiled by the National Antimicrobial Resistance Surveillance Network (NARS-Net) demonstrate a similar trend, with *E. coli* accounting for a substantial proportion of resistant clinical isolates [5]. The widespread distribution of *E. coli*, particularly in urinary tract infections, sepsis, and hospital-acquired infections, underscores its role as both a pathogen and a vector for the dissemination of resistance genes. A significant cause of β-lactam antibiotic resistance in *E. coli* and other *Enterobacteriaceae* is the NDM-1 (New Delhi metallo-β-lactamase-1) enzyme, which was initially documented in 2008 in a Swedish patient with a history of hospitalization in India [6]. Produced by the plasmid-borne blaNDM-1 gene, this enzyme hydrolyzes a broad range of β-lactam antibiotics, including penicillins, cephalosporins, monobactams, and carbapenems, thereby rendering them ineffective [7,8]. The mobility of the blaNDM-1 gene via plasmid-mediated horizontal transfer contributes significantly to its rapid global dissemination. The co-occurrence of NDM-1 with other resistance determinants in clinical isolates further complicates treatment, as these bacteria often exhibit multidrug-resistant (MDR) phenotypes. Currently, no clinically approved inhibitor effectively targets NDM-1, although several candidate molecules are in various stages of preclinical or clinical development [9]. Existing inhibitor strategies include zinc ion chelators (e.g., EDTA, DPA), substrate-binding site inhibitors (e.g., pterostilbene, 3-bromopyruvate), and dual-action molecules that engage both catalytic residues and metal cofactors (e.g., cyclic boronates and thioamides) [10-12]. Despite their potential, many of these compounds face limitations due to poor selectivity, cytotoxicity, or the risk of resistance development. In light of these limitations, attention has increasingly turned to plant-derived products as viable alternatives for novel antimicrobial drug discovery. Natural compounds, particularly phytochemicals from medicinal plants, constitute a vast, chemically diverse repository of bioactive molecules with reported antimicrobial, anti-inflammatory, and antioxidant properties [13,14]. It is estimated that approximately 70-80% of the global population believes in traditional medicine, much of which is based on plant-derived therapies [15]. India, recognized as a global hub of ethnobotanical wealth, hosts more than 20,000 medicinal plant species and is often referred to as the “Botanical Garden of the World” [16,17]. Phytochemicals such as flavonoids, alkaloids, terpenoids, polyphenols, and coumarins have been extensively studied for their role in modulating enzymatic activity and interacting with microbial targets. The integration of computational tools in the drug discovery pipeline has significantly enhanced the efficiency and precision of identifying promising natural inhibitors. Among these, molecular docking stands as a central methodology for virtual screening, enabling the prediction of ligand binding modes and affinities to biological targets [18]. Prior studies have demonstrated that several phytochemicals, including guggulsterone E, β-sitosterol, and withaferin A, possess higher binding stability toward NDM-1 than some standard antibiotics [19]. Catechin-based compounds have also shown notable docking scores and interaction stability [20], while hesperidin has been reported to bind selectively to the functional site of NDM-1 [21]. These *in silico* findings underscore the therapeutic potential of medicinal plant-derived compounds in counteracting NDM-1-mediated resistance. In addition to computational validation, *in vitro* assays such as enzyme inhibition and antibacterial susceptibility testing are essential for

confirming the biological activity of candidate compounds. Several plant-derived molecules, including baicalin, mangiferin, ursolic acid, and curcumin, have demonstrated inhibitory effects on NDM-1 as well as broad-spectrum antimicrobial activity [22-24]. These dual-functional properties, enzyme inhibition and antimicrobial efficacy, render phytochemicals particularly attractive for further pharmacological development. Another vital consideration in drug development is the assessment of pharmacokinetic and safety profiles. The ADMET (absorption, distribution, metabolism, excretion, and toxicity) framework provides a comprehensive evaluation of drug-likeness, helping to reduce late-stage clinical trial failures [25]. Synthetic molecules often fail in clinical settings due to toxicity, lack of selectivity, or metabolic instability. Conversely, while natural compounds are typically safer, they may suffer from limited bioavailability or solubility, requiring structural optimization or formulation strategies to enhance their clinical potential. Bridging this gap needs an interdisciplinary approach that combines ethnopharmacological knowledge with advanced computational and experimental methodologies. Accordingly, the current investigation was undertaken to investigate and validate phytoconstituents with potential inhibitory activity against NDM-1 using an integrative *in silico-in vitro* approach. This study aims to contribute to the global effort to discover novel, safe, and effective therapeutic agents that mitigate the growing threat posed by NDM-1-mediated antibiotic resistance.

2. **Materials and Methods**

2.1. Materials.

All solvents used for extraction and phytochemical analysis were of analytical grade and procured from Merck. Nitrocefin and catechin were purchased from Sigma-Aldrich. Standard antibiotics were obtained from HiMedia Laboratories. An NDM-1-producing *E. coli* strain (ATCC BAA-2469), originally derived from *E. coli* (Migula) Castellani and Chalmers, was procured from Microbiologics (Catalog No. 01113P). Bacterial revival was conducted using sterilized Tryptic Soy Agar (TSA; Soybean Casein Digest Agar). The KWIK-STIK format of the ATCC BAA-2469 strain was activated and cultured on TSA plates, followed by incubation at 37°C for 24 hours. Subsequently, the revived bacterial cultures were maintained on TSA slants and plates for further experimental use.

2.2. Extract preparation.

The medicinal plants selected for the present study, *Acacia arabica*, *Azadirachta indica*, *Ocimum sanctum*, *Commiphora wightii*, and *Tinospora cordifolia*, were chosen based on their extensive use in traditional Indian medicine and strong scientific evidence supporting their antimicrobial and bioactive potential (Table 1). *A. arabica* is rich in polyphenols, particularly catechins and galloylated flavonoids, which have been reported to exhibit antibacterial and enzyme-inhibitory activities [26,27]. *A. indica* is well known for its broad-spectrum antimicrobial properties attributed to limonoids and flavonoids [28,29]. *O. sanctum* possesses phenolic compounds and essential oils with proven antibacterial and resistance-modulating effects [30,31]. *C. wightii* contains guggulsterones and terpenoids reported to interfere with microbial growth and resistance mechanisms [32,33], while *T. cordifolia* is recognized for its immunomodulatory and antimicrobial properties due to alkaloids and diterpenoid lactones [34,35]. Young, healthy parts of the selected medicinal plants were procured from Herbal Park at Chaudhary Devi Lal University, Sirsa, Haryana (India), as well as from local areas/markets

in the Hisar and Sirsa Districts of Haryana (India), and rinsed thoroughly with distilled water to remove any surface contaminants. After cleaning, the plant materials were cut into small pieces and air-dried at ambient temperature for two weeks. Once completely dried, the plant parts were ground into a fine powder using an electric grinder. The powdered material was stored in airtight containers until further extraction by maceration. Finely powdered plant material was soaked in an appropriate solvent and maintained at room temperature for 72-96 hours with continuous shaking to enhance extraction efficiency. The mixture was then filtered using Whatman No. 1 filter paper to remove plant residues. The obtained filtrates were subjected to solvent evaporation under reduced pressure to yield crude or powdered extracts. The final extracts were appropriately labeled and stored at 4°C in a refrigerator until further use [36-38].

Table 1. List of selected medicinal plants.

Sr. No.	Plant name	Common name	Family	Parts collected
1	Acacia arabica (Lam.) Willd.	Babul	Fabaceae	Fruits
2	*Azadirachta indica* A. Juss.	Neem	Meliaceae	Leaves
3	*Ocimum sanctum* L.	Tulsi	Lamiaceae	Leaves
4	*Commiphora wightii* (Arn.) Bhandari	Guggul	Burseraceae	Gum
5	*Tinospora cordifolia* (Thunb.) Miers	Giloy	Menispermaceae	Stem

2.3. In vitro antibacterial activity against NDM-1 active E. coli strain.

The antibacterial assay was performed as per the protocol developed by Zaidan *et al*. using a slightly modified Disk Diffusion Assay (DDA) [39]. The pure cultures of NDM-1 active *E. coli* strains were sub-cultured on Tryptic Soy Agar, and after that, from a pure culture, bacterial colonies were transferred to Tryptic Soy Broth. Then, the broth was incubated for 24 hrs at 37°C for inoculum preparation. The bacterial cultures were grown to 0.5 McFarland standards [40]. Using a sterile cotton swab stick, dip the stick in freshly prepared culture and streak it on freshly prepared Tryptic Soy Agar. During the streaking procedure, the plate was rotated by 60°, and the rubbing procedure was repeated. It was repeated twice for the proper distribution of the inoculum. The inoculated plates were allowed to dry for 4-5 minutes for absorption of excess moisture. Four distinct concentrations of plant extracts were prepared in DMSO (10 mg/ml, 20 mg/ml, 30 mg/ml, and 40 mg/ml). Approximately 6 mm-diameter, well-sterilized disks were used to load the solution. The disks were loaded with amoxicillin and four different selected concentrations of the plant extracts (10 µl/disk), DMSO (10 µl/disk), and EDTA (10 µl/disk). For twenty-four hours, the culture plates were incubated at 37°C. The Hi Antibiotic Zone Scale™ (HiMedia Laboratories, India) was used to assess the zones of inhibition [41]. Every experiment was carried out in triplicate (n = 3), and the results were represented as mean ± standard deviation (SD). The antibacterial activity data were statistically analyzed using two-way analysis of variance (ANOVA) to determine significance compared to the control group, employing GraphPad Prism for Windows (Version 6.01, GraphPad Software Inc., San Diego, California, USA). A p-value of less than 0.05 ($p < 0.05$) was determined to be statistically significant.

2.4. Design of the database of phytoconstituents.

The database of phytoconstituents for the selected medicinal plant was carefully compiled from available literature and databases, including PubChem [42]. A thorough literature review was conducted, along with an in-depth exploration of relevant databases such as PubChem, to gather information on the plant's phytoconstituents. The primary

phytochemical constituents were identified and compiled, referencing the detailed data available on PubChem. PubChem provided an extensive list of known phytoconstituents for these plants, including molecular structures, properties, and other key characteristics. When specific compound structures were unavailable in PubChem, ChemSketch (ACD Labs) was used to draw the structures.

2.5. In silico prediction of pharmacokinetics.

In silico pharmacokinetic predictions were carried out to evaluate the drug-likeness of the phytoconstituents of selected medicinal plants. For this purpose, SwissADME (a web-based tool; http://www.swissadme.ch/) was used to predict key pharmacokinetic properties of the phytoconstituents (the SMILES of all ligands were entered to obtain results). SwissADME is a comprehensive online tool for evaluating the pharmacokinetic profiles of small molecules based on their chemical structures [43]. Based on the predictions of these parameters, the most promising compounds were selected as potential drug candidates. The compounds with favorable pharmacokinetic profiles were thus finalized as ligands for subsequent stages of the research [44].

2.6. In silico screening of the phytoconstituents against NDM-1.

Molecular docking was performed to evaluate binding interactions between the optimized phytoconstituents and the NDM-1 protein. These studies were carried out using AutoDock Vina [45]. The crystal structure of NDM-1 (PDB ID: 4U4L) was retrieved from the Protein Data Bank (https://www.rcsb.org) [46]. The crystal structure was prepared by removing existing ligands, water molecules, unbound ions, and extra chains using the PyMOL molecular graphics tool (Schrödinger, LLC). Thereafter, non-polar hydrogens were merged, and polar hydrogens were added to the protein using AutoDock Tools [47]. The prepared structure was saved in docking-ready PDBQT format. Two-dimensional (2D) chemical structures of all ligands (standard as well as test compounds) were drawn using MarvinSketch 18.5.0 (ChemAxon Ltd.) and converted into three-dimensional (3D) conformations (mol2 format) using the Frog2 server [48]. Polar hydrogens were added, non-polar hydrogens were merged with carbons, and the internal degrees of freedom and torsions were defined. The ligand files were subsequently saved in PDBQT format using AutoDock Tools [47]. The docking grid was centered at X = 37.629, Y = -41.340, and Z = -31.009, with a grid box dimension of 40 × 40 × 40 Å, ensuring complete coverage of the catalytic active site and surrounding residues of the NDM-1 protein, including the Zn^{2+}-binding region. An exhaustiveness value of 8 was employed during docking to balance computational efficiency with adequate conformational sampling. To validate the docking protocol, the co-crystallized ligand present in the NDM-1 crystal structure (PDB ID: 4U4L) was re-docked into the active site using identical grid parameters. The binding pose of the re-docked ligand was compared with its crystallographic conformation (PDB ID: 4U4L), and the protocol was considered reliable based on the reproduction of a similar binding orientation with an RMSD value within the acceptable threshold (< 2.0 Å), thereby confirming the accuracy of the docking setup and binding site definition. Subsequently, the 3D-optimized phytoconstituents were docked into the validated NDM-1 binding site and ranked using the AutoDock Vina scoring function. The binding free energy values (ΔG, kcal/mol) were obtained from the log files, and the protein-ligand interaction profiles were analyzed using PyMOL (Schrödinger, LLC) and Discovery Studio

Visualizer (Dassault Systèmes BIOVIA).

2.7. In vitro evaluation of the most active phytoconstituents against the NDM-1 active bacterial strain.

Based on the results of the molecular docking analysis, the most promising phytoconstituent (catechin) was tested against the NDM-1 active *E. coli* bacterial strain using modified DDA [39].

2.8. In silico toxicity evaluation of the most active phytoconstituent.

In silico toxicity profiling of the most active phytoconstituent (catechin) was carried out using pkCSM [49,50].

3. Results and Discussion

3.1. Antibacterial activity of different plant extracts against the NDM-1 active E. coli strain.

Antibacterial activity of different plant extracts was investigated after 24 hrs. Out of 5 plants, only A. arabica (Lam.) Willd. have shown the inhibitory action against the NDM-1 active *E. coli* strain (Table 2). In case of *A. arabica (Lam.) Wild*, all extracts showed considerable activity with the diameter of inhibition zones ranging from 8 to 16 (Table 3) against the NDM-1 active *E. coli*. Acetone, ethanol, and water extract of *A. arabica (Lam.) Willd* showed antibacterial activity against NDM-1 active *E. coli*, and the zone of inhibition increased with an increase in concentration of plant extract. Acetone extract of *A. arabica (Lam.) Willd* showed the maximum zone of inhibition compared to ethanol and water extracts of *A. arabica (Lam.) Wild.*

Table 2. *In vitro* evaluation of the medicinal plants against the NDM-1-producing *E. coli* strain.

Sr. No.	Name of the Plant	Acetone Extract	Ethanol Extract	Water Extract
1	A. arabica (Lam.) Willd.	+	+	+
2	*A. indica* A. Juss.	-	-	-
3	*O. sanctum* L.	-	-	-
4	*C. wightii* (Arn.) Bhandari	-	-	-
5	*T. cordifolia* (Thunb.) Miers	-	-	-

Table 3. Zone of inhibition of different extracts of *A. arabica* (Lam.) Wild. against NDM-1 active *E. coli.*

Extract	Zone of inhibition in diameter (mm)				
	10 mg/ml	20 mg/ml	30 mg/ml	40 mg/ml	Std. (EDTA)
Water	--	8.66±1.15 ^{a}	12.66±1.15^{ab}	14.00±2.00 ^{ab}	20.00±2.30 ^{abcd}
Ethanol	--	11.33±2.30 ^{a}	14.00±2.00 ^{ab}	15.00±2.00 ^{ab}	20.66±1.15 ^{abcd}
Acetone	8.00±0.00	12.00±0.00 ^{a}	14.00±0.00 ^{a}	16.00±0.00 ^{ab}	20.66±1.15 ^{abc}

All the values are mean ± SD (n = 3). Data was statistically significant (2-Way ANOVA): a = $p < 0.05$ vs 10 mg/ml; b = $p < 0.05$ vs 20 mg/ml; c = $p < 0.05$ vs 30 mg/ml; d = $p < 0.05$ vs 40 mg/ml.

3.2. Antibacterial activity of different plant extracts against the NDM-1 active E. coli strain.

Synergistic antibacterial effects of different plant extracts and amoxicillin were determined using DDA with slight modifications and assessed after 24 hrs. Only A. arabica (Lam.) Willd. have shown the inhibitory action with amoxicillin against the NDM-1 active *E. coli* strain (Table 4).

Table 4. *In vitro* evaluation of the medicinal plants against NDM-1-producing *E. coli* strain in combination with amoxicillin.

Sr. No.	Name of the plant	Acetone extract + amoxicillin	Ethanol extract + amoxicillin	Water extract + Amoxicillin
1	A. arabica (Lam.) Willd.	+	+	+
2	*A. indica* A. Juss.	-	-	-
3	*O. sanctum* L.	-	-	-
4	*C. wightii* (Arn.) Bhandari	-	-	-
5	*T. cordifolia* (Thunb.) Miers	-	-	-

3.3. Synergistic effect of different extracts of A. arabica (Lam.) Wild. and Amoxicillin against NDM-1 active E. coli.

Extracts of A. arabica (Lam.) Willd. (Figure 1) in combination with amoxicillin, showed synergistic effect with an increase in inhibition zones measured within a range of 11.67 to 19.00 mm against NDM-1 active *E. coli* (Table 5). Notably, the zone of inhibition increased with higher concentrations of the extracts. However, the acetone extract showed higher antibacterial activity as compared to ethanol and water extracts.

(a) **(b)** **(c)**

Figure 1. Synergistic effect of **(a)** acetone; **(b)** ethanol; **(c)** water extracts of A. arabica (Lam.) Willd. + amoxicillin at different concentrations.

Table 5. Synergistic effect of *A. arabica* (Lam.) Wild. against NDM-1 active *E. coli* in combination with amoxicillin.

Extract	Zone of Inhibition in Diameter (mm)					
	Ab	10 mg/ml + Ab	20 mg/ml + Ab	30 mg/ml + Ab	40 mg/ml + Ab	Std. (EDTA)
Water	10.33±0.88	11.67±1.20	13±1.15 ^{a}	14.00±1.15 ^{ab}	14.67±0.88 ^{abc}	24.33±1.33 ^{abcde}
Ethanol	11.00±0.00	12.00±0.00 ^{a}	13.33±0.33 ^{a}	15.00±0.58 ^{ab}	17.67±0.67 ^{abc}	25.00±0.58 ^{abcde}
Acetone	10.67±0.33	12.67±0.33 ^{a}	13.67±0.33 ^{a}	15.00±0.58 ^{ab}	19.00±0.58 ^{abcd}	26.67±0.33 ^{abcde}

All the values are mean ± SD (n = 3). Data was statistically significant: a = $p < 0.05$ vs Ab; b = $p < 0.05$ vs 10 mg/ml + Ab; c = $p < 0.05$ vs 20 mg/ml + Ab; d = $p < 0.05$ vs 30 mg/ml + Ab; e = $p < 0.05$ vs 40 mg/ml + Ab.

MIC values of amoxicillin and extracts were determined at various concentrations. MIC value for amoxicillin was in the range of 100-120 µg/ml, and MIC values of acetone, ethanol, and water extracts for *A. arabica* (Lam.) Willd. were in the range of 3-6 mg/ml against NDM-1 active *E. coli*.

3.4. In silico screening of phytoconstituents of A. arabica (Lam.) Willd. against NDM-1.

3.4.1. Designing a database of phytoconstituents of *A. arabica* (Lam.) Willd.

The database of phytoconstituents of *A. arabica* (Lam.) Willd. was compiled based on an extensive literature review. The database was generated utilizing PubChem. ChemSketch was employed to draw their structures (Table S1).

3.4.2. *In silico* prediction of pharmacokinetics of the phytoconstituents.

In silico methods play a vital role in the early stages of drug discovery, particularly in predicting the pharmacokinetic behavior of compounds (absorption, distribution, metabolism, and excretion (ADME)). These methods rely on theoretically derived statistical and machine learning models that simulate how a compound might behave in the human body, thereby reducing the need for extensive *in vitro* and *in vivo* studies in the initial phases [51]. SwissADME calculates important parameters such as gastrointestinal (GI) absorption, blood-brain barrier (BBB) permeability, P-glycoprotein (P-gp) substrate identification, cytochrome P450 (CYP450) enzyme inhibition, and skin permeability (Log Kp), among others. According to Lipinski's rule, a compound is more likely to exhibit good oral bioavailability if it meets the following criteria: molecular weight (Mol. Wt.) ≤ 500 Da; LogP (octanol-water partition coefficient) ≤ 5; number of hydrogen bond donors (HBDs) ≤ 5; number of hydrogen bond acceptors (HBAs) ≤ 10 [52]. Compounds that conform to these rules are generally considered to have favorable pharmacokinetic properties and are more likely to succeed as orally active drug candidates. *In silico* pharmacokinetic predictions were performed to evaluate the drug-likeness of phytoconstituents derived from *A. arabica* (Lam.) Willd. using web-based platforms such as SwissADME [43]. A total of 165 compounds were initially assessed based on Lipinski's Rule of Five [52]. Detailed information on these compounds is provided in Table S2. From this initial set, 76 plant-derived compounds met the selection criteria and were subsequently chosen as potential ligands for molecular docking studies.

3.4.3. *In silico* screening of the phytoconstituents against bacterial protein (NDM-1)

In silico methods play a vital role in the early stages of drug discovery, particularly in predicting the pharmacokinetic behavior of compounds (absorption, distribution, metabolism, and excretion (ADME)). These methods rely on theoretically derived statistical and machine learning models that simulate how a compound might behave in the human body, thereby reducing the need for extensive *in vitro* and *in vivo* studies in the initial phases [51]. SwissADME calculates important parameters such as gastrointestinal (GI) absorption, blood-brain barrier (BBB) permeability, P-glycoprotein (P-gp) substrate identification, cytochrome P450 (CYP450) enzyme inhibition, and skin permeability (Log Kp), among others. According to Lipinski's rule, a compound is more likely to exhibit good oral bioavailability if it meets the following criteria: molecular weight (Mol. Wt.) ≤ 500 Da; LogP (octanol-water partition coefficient) ≤ 5; number of hydrogen bond donors (HBDs) ≤ 5; number of hydrogen bond acceptors (HBAs) ≤ 10 [52]. Compounds that conform to these rules are generally considered to have favorable pharmacokinetic properties and are more likely to succeed as orally active drug candidates. *In silico* pharmacokinetic predictions were performed to evaluate the drug-likeness of phytoconstituents derived from *A. arabica* (Lam.) Willd. using web-based platforms such as SwissADME [43]. A total of 165 compounds were initially assessed based on Lipinski's Rule of Five [52]. Detailed information on these compounds is provided in Table S2. From this initial set, 76 plant-derived compounds met the selection criteria and were subsequently chosen as potential ligands for molecular docking studies.

3.4.4. *In silico* screening of the phytoconstituents against bacterial protein (NDM-1).

In silico virtual screening has emerged as a powerful and cost-effective strategy for identifying potential therapeutic candidates by rapidly predicting molecular interactions

between target proteins and ligands [53,54]. *In silico* screening of various photochemicals was performed with bacterial NDM-1 enzyme (PDB ID: 4U4L). The docking procedure was initially validated through redocking of the co-crystallized ligand of NDM-1 (PDB ID: 4U4L). The RMSD between the docked pose and the crystallographic conformation was calculated using AutoDockTools and found to be < 2.0 Å, confirming the reliability of the docking protocol. The re-docked ligand of NDM-1 (PDB ID: 4U4L) produced a pose similar to that of the co-crystallized inhibitor with NDM-1 (with ΔG = -7.6 kcal/mol), indicating that a rational docking protocol was used in this study (Figure S1). On the basis of Lipinski's rule of five, 89 compounds were excluded due to Lipinski's violation, and only 76 compounds were screened against NDM-1, and 30 compounds showed appreciable results in the molecular docking study (Table 6).

Table 6. *In silico* docking results of various compounds of *A. arabica* (Lam.) Willd. against the NDM-1 protein.

Comp. Code	ΔG	Hydrogen bonds (bond length)	Hydrophobic bonds and other interactions
A1	-4.4	Asp124 (3.04 Å), Asn220 (2.82, 2.90 Å)	Zn301, Zn302
A3	-6.4	Gln123 (2.84, 3.03 Å), Asp124 (3.32 Å), Lys211 (2.97 Å)	His122, Zn302, His189, Asn220
A6	-6.8	Asp124 (3.92 Å), Gln123 (2.97 Å), Asn220 (3.38 Å), Lys211 (3.03 Å)	Trp93, His122, His250, Zn301
A7	-6.4	Asp212 (3.74 Å), Ser251 (3.07, 3.09 Å), Lys211 (3.18 Å)	His250, Ala215, Zn301, Lys211
A14	-5.0	Asp124 (3.08 Å)	Trp93, Val73, His250, Lys211, Zn302
A20	-4.6	Asp124 (3.02, 2.96 Å), Asn220 (2.98, 3.05, 3.13 Å)	Zn301, Zn302
A21	-4.5	Asp124 (2.92 Å), Asn220 (3.21, 3.01 Å)	Zn301, Zn302
A30	-6.9	Lys211 (3.23 Å)	His122, Val73, Trp93, Leu65, His250, Asp66, His189
A34	-5.2	Asp124 (3.07 Å)	Trp93, Zn302
A35	-6.8	Lys211 (3.04 Å), Gln123 (2.87 Å)	Trp93, Zn302, Asp124, Asn220
A56	-4.9	Asp124 (3.17 Å), Gln123 (3.14, 3.11 Å), Asn220 (3.00, 3.18 Å)	His122, Zn302, His189
A80	-6.6	Asp124 (3.08 Å)	His189, His250, Val73, Trp93, Leu65, Zn301, Zn302
A86	-3.6	Asp124 (3.02 Å)	Zn302
A97	-4.5	Asp124 (3.08 Å), Ser217 (3.86 Å)	His250, Val73, Trp93, Ala215, Lys211, Zn302
A98	-4.7	Lys211 (3.13 Å)	His122, Trp93, Val73, Zn302, His189
A99	-4.9	Lys211 (3.31 Å)	Trp93, Val73, His250, Lys211, Ala215, Zn301, Zn302
A117	-5.0	Asp124 (3.02 Å)	Trp93, His122, His189, His250, Lys211, Ala215, Val73, Zn301, Zn302
A118	-5.4	-	His250, His189, Trp93, His122, Zn302
A123	-5.7	-	His250, His189, Trp93, His122, Val73(4.60), Zn301
A127	-6.0	-	His250, Trp93, His122, Val73, Zn301
A128	-5.7	Asp124 (3.74 Å), Gln123 (2.92 Å)	His250, His189, Trp93, His122
A134	-5.5	Gln123 (2.98 Å)	His250, His189, Trp93, His122, Val73, Leu65, Zn301, Zn302
A147	-4.8	-	Trp93, Zn302
A149	-5.1	-	Trp93, His122, Zn302
A150	-5.1	-	Trp93, His122, Val73, Zn302
A161	-5.7	Asp124 (3.29, 3.08 Å), Asn220 (3.38 Å)	His250, Val73, Zn302, His122
A162	-5.9	Asp223 (4.79 Å)	His250, Zn301, Zn302
A163	-5.2	Asp124 (2.93, 3.63 Å), Asn220 (2.97 Å), Gln123 (2.99, 3.17 Å)	Zn302, His122
A164	-4.6	Asp124 (3.63, 3.12 Å), Gln123 (2.98 Å)	Trp93, His250, Zn302
A165	-5.3	Asp124 (3.06 Å)	Trp93, Val73, Zn302, His122
4U4L ligand	-7.6	Asn220 (3.05 Å)	Trp93, His122, His250, Zn301, Zn302

Out of the above-mentioned compounds, catechin (A6) was selected for further in vitro synergistic evaluation with amoxicillin against the NDM-1 active E. coli bacterial strain. This compound was chosen based on minimum binding energy (ΔG) and the maximum number of

hydrogen bonds, hydrophobic interactions, and metal interactions (with Zn^{2+} ion) observed in the molecular docking analysis. Catechin has shown 4 strong hydrogen bonds and metal interaction with Zn301 (Figure 2). The rationale for this selection is that the binding energy (ΔG) indicates the strength of the interaction between the compound and the bacterial protein, while hydrogen bonds and metal interactions play a key role in the stability of the protein-ligand complex. Strong hydrogen bonding and metal interactions help to stabilize the interaction, which is essential for effective inhibition of the bacterial NDM-1 protein.

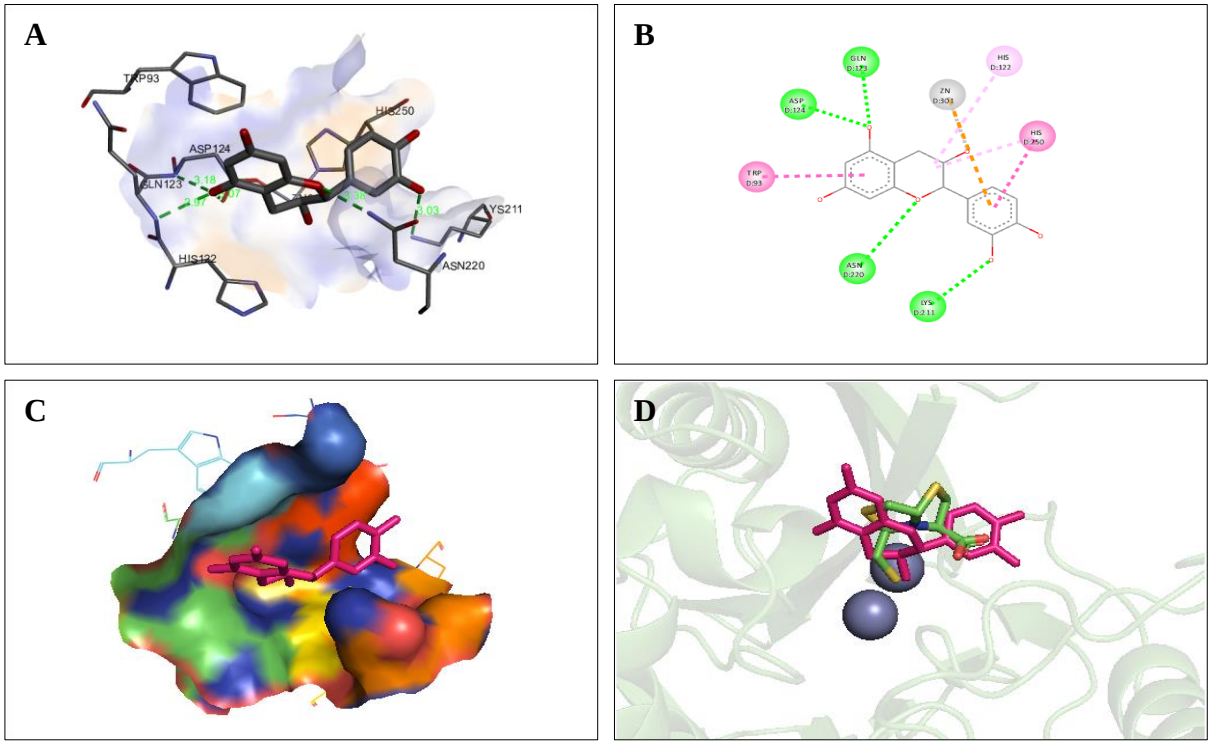

Figure 2. Interaction analysis of catechin (A6) with NDM-1. **(A)** 3D docked pose of catechin showing hydrogen bond interactions; **(B)** 2D docked pose of catechin showing hydrogen bond and hydrophobic interactions; **(C)** Orientation of catechin in the active site of NDM-1; **(D)** Overlay of the docked pose of catechin (pink) with that of the co-crystallized ligand (green).

3.5. In vitro evaluation of catechin against the NDM-1 active E. coli strain.

On the basis of the docking results, the antibacterial activity of catechin was examined against the NDM-1 active *E. coli* bacterial strain using DDA with slight modifications [39]. Catechin (Figure 3) showed a potentiated effect in combination with amoxicillin, with the zone of inhibition ranging from 9.67 to 17.00 mm against NDM-1 *E. coli* (Table 9). The results have shown that the combined effects of catechin in conjunction with amoxicillin exhibit antibacterial potential against NDM-1 active *E. coli*.

Table 7. Effect of catechin in combination with amoxicillin against the NDM-1 active *E. coli* strain.

Compound	Zone of inhibition in diameter (mm)
Ab	8.33±0.33
Catechin (20 µg/ml) + Ab	9.67±0.88 [a]
Catechin (40 µg/ml) + Ab	13.0 ±1.52 [ab]
Catechin (60 µg/ml) + Ab	14.67±1.33 [ab]
Catechin (80 µg/ml) + Ab	17.00±1.00 [abcd]
Std. (EDTA) + Ab	17.33±0.33 [abcde]

All the values are mean ± SD (n = 3). Data was statistically significant: a = $p < 0.05$ vs Ab; b = $p < 0.05$ vs 20 µg/ml + Ab; c = $p < 0.05$ vs 40 µg/ml + Ab; d = $p < 0.05$ vs 60 µg/ml + Ab; e = $p < 0.05$ vs 80 µg/ml + Ab.

Notably, the zone of inhibition increased with higher concentrations of the phytoconstituent. MIC of catechin was in the range of 35-40 µg/ml against NDM-1 *E. coli*.

Figure 3. Synergistic effect of catechin and amoxicillin against the NDM-1 active *E. coli* bacterial strain.

3.6. In silico toxicity prediction of catechin.

Toxicity prediction is a crucial component of early-phase drug discovery, aiming to eliminate candidates with adverse safety profiles before they proceed to costly experimental evaluations. *In silico* tools such as pkCSM enable rapid and cost-effective screening by integrating structural features with known toxicological datasets, thereby predicting how novel molecules might interact with key biological systems. These predictions help guide the selection of compounds with an optimal balance of efficacy and safety, and are particularly valuable in medicinal chemistry programs focused on optimizing lead candidates [55-58]. The pharmacokinetics and potential toxicity profiles for mutagenicity, immunotoxicity, skin irritancy, carcinogenicity, and reproductive toxicity for catechin were systematically assessed using the pkCSM online tool (https://biosig.lab.uq.edu.au/pkcsm/), which employs graph-based signatures to predict various toxicological endpoints [49,50]. Catechin was predicted to have a favorable toxicity profile (Table 8). It is non-mutagenic (negative for AMES test), non-carcinogenic, non-hepatotoxic, and does not induce skin sensitization. It is also predicted not to inhibit hERG channels (I and II), indicating low cardiotoxicity risk. The acute oral toxicity (LD_{50}) and chronic toxicity (LOAEL) values suggest a relatively safe dosage range. Overall, the pkCSM predictions indicate that catechin possesses a favorable pharmacokinetic and toxicity profile, with minimal predicted risks for major adverse effects, making it a promising candidate for further drug development and safety evaluation. These predictions provide valuable insights for prioritizing catechin for further *in vitro* and *in vivo* toxicological assessments.

Table 8. Predicted pharmacokinetics and toxicity for catechin using pkCSM.

Model name	Predicted value
Absorption	
Water solubility (log mol/L)	-3.117
Caco2 permeability (log Papp in 10^{-6} cm/s)	0.283
Intestinal absorption (human) (% Absorbed)	68.829
Skin Permeability (log Kp)	-2.735
P-glycoprotein substrate	Yes
P-glycoprotein I inhibitor	No
P-glycoprotein II inhibitor	No
Distribution	

Model name	Predicted value
VDss (human) (log L/kg)	1.027
Fraction unbound (human) (Fu)	0.235
BBB permeability (log BB)	-1.054
CNS permeability (log PS)	-3.298
Metabolism	
CYP2D6 substrate	No
CYP3A4 substrate	No
CYP1A2 inhibitor	No
CYP2C19 inhibitor	No
CYP2C9 inhibitor	No
CYP2D6 inhibitor	No
CYP3A4 inhibitor	No
Excretion	
Total Clearance (log ml/min/kg)	0.183
Renal OCT2 substrate	No
Toxicity	
AMES toxicity	No
Max. tolerated dose (human) (log mg/kg/day)	0.438
hERG I inhibitor	No
hERG II inhibitor	No
Oral Rat Acute Toxicity (LD_{50}) (mol/kg)	2.428
Oral Rat Chronic Toxicity (LOAEL) (log mg/kg_bw/day)	2.5
Hepatotoxicity	No
Skin Sensitisation	No
T. Pyriformis toxicity (log ug/L)	0.347
Minnow toxicity (log mM)	3.585

3.7. Discussion.

In the present study, 5 medicinal plants were selected for antibacterial potential against the NDM-1 *E. coli* strain. Out of 5 plants, only *A. Arabica* has shown bactericidal activity, with effective concentrations from 10 mg/ml to 40 mg/ml against the NDM-1 active *E. coli*. Acetone, ethanol, and water extracts from *A. Arabica*, along with amoxicillin, demonstrated a synergistic antibacterial effect against the NDM-1-producing *E. coli* strain. The inhibition zones ranged from 8 to 16 mm, indicating the effectiveness of the combined treatment (A. Arabica extracts + amoxicillin) in inhibiting bacterial growth. This synergy suggests that the plant extract may enhance the efficacy of traditional antibiotics against multidrug-resistant bacteria. Among all the extracts tested, the acetone extract produced the largest inhibition zone compared to the ethanol and water extracts. This plant produces a diverse range of bioactive compounds with distinct structures and chemical properties, recognized for their therapeutic potential. These bioactive substances, including alkaloids, coumarins, flavonoids, polyphenols, terpenoids, quinones, and phytosteroids, each contribute to the medicinal properties of these plants and their use in treating a variety of health conditions [13, 59]. Chandar *et al*. reported that extracts from *Combretum albidum* G. Don, *Hibiscus acetosella* Welw. ex Hiern, *Hibiscus cannabinus* L., *Hibiscus furcatus* Willd., *Punica granatum* L., and *Tamarindus indica* L. demonstrated bactericidal activity, with effective concentrations ranging between 5 mg/ml and 15 mg/ml. The MIC values for these extracts were found to be between 2.56 mg/ml and 5.12 mg/ml. These results suggest that plant extracts may have potential as inhibitors of NDM-1 and warrant further exploration for their ability to combat antibiotic-resistant bacterial strains [60]. Inbaraj (2014) investigated the antibacterial properties of the leaf extract from *Lantana camara* Linn. (LELC) in combination with gentamicin and ceftriaxone against Gram-negative bacteria, including *E. coli* (ATCC 25922), *Staphylococcus aureus* (ATCC 25923), and NDM-1-

producing *K. pneumoniae* strains. Results revealed that LELC exhibited inhibitory effects against *E. coli* (3.5 mm), *S. aureus* (4 mm), and NDM-1-producing strains (1.2 mm). Noteworthy synergistic effects were observed: LELC and gentamicin showed enhanced inhibition (5.5 mm) against the *E. coli* strain, while LELC and ceftriaxone showed a stronger effect (6 mm) against *the S. aureus* strain. These findings suggest that plant extracts exhibit significant antibacterial activity against drug-resistant Gram-negative bacteria and could serve as future antimicrobial agents against resistant strains [61]. Molecular docking, a widely used computational method in bioinformatics, is designed to simulate the interaction between two molecules: a smaller molecule, called the ligand, and a larger biomolecule (macromolecule), known as the target, which is typically a protein or DNA [62]. Integrating ADMET evaluation into the early phases of drug discovery enables researchers to identify and address potential issues before advancing candidates to expensive, time-intensive clinical trials. This proactive strategy increases the chances of success and supports the development of safer, more effective therapeutic agents. In this study, only one compound (catechin) from *A. Arabica* was selected for further *in vitro* evaluation. This compound was found to have more stable binding energy (ΔG), i.e., -6.8 kcal/mol. Hydrogen bonding was also present in the ligand-protein complex, which contributed to its stability. Various interactions, such as hydrophobic and metal interactions, were also reported in the *in silico* screening. Several studies provided information on molecular docking, with a focus on docking affinities and cytotoxic activities of various compounds against specific protein targets. Salari-jazi *et al*. (2021) investigated binding interactions of catechin-based compounds, NPC18185, NPC98583, NPC100251, NPC112380, and NPC171932 against NDM-1 with significant binding energies, ranging from -22.0 to -24.3 kcal/mol and Glide XP Scores from -7.78 to -13.95 kcal/mol [20]. Rahman and Khan evaluated natural substances from the ZINC database and well-known antibiotics using molecular docking and dynamics against NDM-1 [19]. Natural substances such as guggulsterone E, aristolochic acid, β-sitosterol, withaferin A, and diosgenin demonstrated stable binding interactions. Shi *et al*. screened a compound library containing 2,177 natural substances using virtual screening techniques against NDM-1. Six compounds (ginsenoside, stevioside, hesperidin, diosmin, paromomycin, and rutin) showed promising inhibitory activity against NDM-1. The most potent of these was hesperidin, with an IC_{50} value of 3.348 ± 1.35 pM. Hesperidin was found to specifically interact with key residues in the active site of NDM-1 [21]. Vasudevan *et al*. evaluated natural substances from Dr. Duke's Phytochemical and Ethnobotanical Database using molecular docking. Ten of these compounds exhibited Glide scores ranging from -9.44 to -5.52. Mangiferin and withaferin A emerged as promising NDM-1 inhibitors. Virtual screening was employed to select 2,400 compounds (each having at least 80% similarity to D-captopril) from the PubChem database. The lead compounds, identified by PubChem IDs 53986787, 20011444, 44273312, 20052521, 18234368, 54290970, 10736252, 57322631, and 163066, exhibited strong binding affinities ranging from -9.1 kcal/mol to -6.7 kcal/mol [63]. Barman *et al*. evaluated 22 plant-based compounds for their inhibitory efficacy against NDM-1 through molecular docking. Molecular docking studies indicated that garcinol was the most promising NDM-1 inhibitor; however, a quantitative structure-activity relationship study predicted ajugasterone-C with the lowest MIC [64]. Chetia *et al*. identified echitaminic acid, isoboonein, scholaracine, kaempferol, M-coumaric acid, N-feruloyl tyramine, norwedelic acid, alpha-pinene, rosmarinic acid, carvacrol, beta-ocimene, andrographolide, piperine, linalyl acetate, luvangetin, psoralen, and gamma-fagarine with favorable drug-like properties and binding energies ranged from -7.12 to -4.56 kcal/mol. With

a binding energy of -7.12 kcal/mol, piperine was the most effective NDM-1 inhibitor [65]. Bibi *et al*. identified butein, rosmarinic acid, and monodemethylcurcumin as potential inhibitors of NDM-1 through molecular docking [66]. Assaf *et al*. (2023) identified ursolic acid as a potent inhibitor of NDM-1 via virtual screening [67]. Muhammad *et al*. (2018) investigated diaporthein A and diaporthein B, using computational ligand-target docking methods with binding energies of -8.02 and -8.41 kcal/mol, respectively [68]. Etminani *et al*. identified 3,7-dimethyloct-1,5-dien-3,7-diol from *Ocimum basilicum* (-6.43 kcal/mol), α-terpineol from *Rosmarinus officinalis* and *Thymus vulgaris* (-6.32 kcal/mol), and carvotanacetone from *Eucalyptus globulus* (-6.54 kcal/mol) as potent NDM-1 inhibitors [69]. Hemlata *et al*. identified ellagic acid as a potent inhibitor of β-lactamase using *in silico* and *in vitro* methods with an XP docking score of ≤ -6 kcal/mol and MIC value of 300 µg against *Kluyvera georgiana* strains [70]. Diaz *et al*. identified N-methyl mycosporine-Ser as a strong inhibitor of B1-MBLs using a pharmacophore-based approach and high-throughput virtual screening [71]. Fatima *et al*. screened a total of 102 phytochemicals from 10 medicinal plants [72]. Thakur *et al*. identified didymellamide and makaluvic acid as potential inhibitors of B1-MBLs using a pharmacophore-based method [73]. Horie *et al*. (2018) identified soysaponin V as a potent inhibitor of β-lactamase [74]. Ning *et al*. identified embelin as a potent inhibitor of NDM-1 with an IC_{50} of 2.1 µM. The hydroxyl group of the embelin molecule was firmly anchored in the NDM-1 active site, where it directly interacted with the Zn^{2+} metal ion [75]. Baicalin was found to restore the susceptibility of *E. coli* to β-lactam antibiotics by efficiently inhibiting NDM-1, with IC_{50} values of 3.89 µM. Molecular modeling studies revealed that baicalin binds to the Zn^{2+} ion in the active site of NDM-1 and forms hydrogen bonds with key residues, stabilizing the complex structure [76]. These studies highlight the potential of various compounds to inhibit protein targets involved in disease pathways, with several showing significant docking scores, indicating strong binding affinities. Hence, catechin has the potential to be a lead molecule and was tested in synergy with amoxicillin against the NDM-1 active *E. coli* strain to evaluate its potential as part of a combination therapy. The *in vitro* assay results suggest that catechin exhibits antibacterial activity against NDM-1-producing *E. coli* when tested in combination with amoxicillin using modified DDA. The zone of inhibition of amoxicillin was increased from 8.33 mm to 17.00 mm by catechin (at 80 µg/ml concentration). The research findings highlight that the catechin, when used with amoxicillin, effectively inhibits the growth of NDM-1-producing *E. coli*. Additionally, as catechin concentration increased, the zone of inhibition widened. This indicates that the combination's activity is dose-dependent, underscoring its potential to enhance amoxicillin's efficacy against resistant bacterial strains.

4. Conclusions

This study addresses the pressing global challenge of AMR, with a particular focus on *E. coli* strains producing NDM-1, a major obstacle in current infectious disease management. Employing a comprehensive approach that integrates in vitro assays with in silico molecular docking techniques, the research evaluated the synergistic potential of phytoconstituents isolated from selected medicinal plants. Of the 5 plants initially screened, A. arabica demonstrated the most significant antibacterial activity, particularly when combined with amoxicillin. Acetone extracts consistently exhibited the largest zones of inhibition, suggesting a notable enhancement of antibiotic efficacy through synergistic interactions. The MICs of the acetone extract, in conjunction with its potentiating effects on amoxicillin, underscore its potential as an adjunct therapy against drug-resistant bacterial strains. Further computational

analysis identified catechin as the lead phytoconstituent, based on its favorable binding affinity, stable interactions with key catalytic residues, and coordination with the Zn^{2+} ions within the NDM-1 active site. These *in silico* predictions were substantiated by *in vitro* assays, which confirmed the enhanced antibacterial activity of amoxicillin when co-administered with catechin. Overall, the findings highlight catechin as a promising candidate for the development of novel, plant-based antibacterial agents targeting resistant pathogens. These findings contribute valuable insights into the potential of phytochemicals as resistance-modulating agents and support their further exploration in the context of AMR. While the present study provides compelling evidence for the resistance-modulating potential of catechin against NDM-1-producing *E. coli*, certain limitations should be acknowledged. First, the experimental validation was restricted to in vitro antibacterial assays and in silico docking analyses, and detailed enzyme kinetics, molecular dynamics simulations, and *in vivo* efficacy studies were beyond the scope of the current investigation. Second, although the synergistic effect of catechin with amoxicillin was clearly demonstrated, structure-activity relationship optimization and formulation studies were not undertaken at this stage. Future work should focus on elucidating the precise mechanism of NDM-1 inhibition through enzymatic and kinetic analyses, assessing binding stability via molecular dynamics simulations, optimizing catechin-based derivatives for improved potency and bioavailability, and conducting in vivo pharmacokinetic and toxicity evaluations.

Supplementary Materials

Additional experimental data can be found in Figure S1, Table S1 and Table S2 in the Supplementary Materials.

Author Contributions

Conceptualization, A.S.G. and S.K.G.; formal analysis, A.K. and A.S.G.; data curation, A.K. and S.R.; writing—original draft preparation, A.K., A.S.G., and S.K.G.; writing—review and editing, A.K., A.S.G., S.K.G., and S.R. All authors have read and agreed to the published version of the manuscript.

Institutional Review Board Statement

Not applicable.

Informed Consent Statement

Not applicable.

Data Availability Statement

No new data were created or analyzed in this study. Data sharing is not applicable.

Funding

No funding was received for conducting this study.

Acknowledgments

The authors gratefully acknowledge the laboratory and technical support provided by the Department of Biotechnology, Chaudhary Devi Lal University, Sirsa, Haryana, India, for conducting this research work.

Conflicts of Interest

The authors declare no conflict of interest.

Role of Funders

No funding was received for conducting this study.

Abbreviations

The following abbreviations are used in this manuscript:

Abbreviation	Definition
ADME	Absorption, Distribution, Metabolism, and Excretion
ADMET	Absorption, Distribution, Metabolism, Excretion, and Toxicity
AMR	Antimicrobial Resistance
ANOVA	Analysis of Variance
ATCC	American Type Culture Collection
BBB	Blood-Brain Barrier
CNS	Central Nervous System
CYP450	Cytochrome P450
DDA	Disk Diffusion Assay
DMSO	Dimethyl Sulfoxide
E. coli	*Escherichia coli*
EDTA	Ethylenediaminetetraacetic Acid
GI	Gastrointestinal
GLASS	Global Antimicrobial Resistance and Use Surveillance System
HBA	Hydrogen Bond Acceptor
HBD	Hydrogen Bond Donor
hERG	Human Ether-à-go-go-Related Gene
IC_{50}	Half Maximal Inhibitory Concentration
LD_{50}	Median Lethal Dose
LOAEL	Lowest Observed Adverse Effect Level
MBLs	Metallo-β-Lactamases
MDR	Multidrug Resistant
MIC	Minimum Inhibitory Concentration
Mol. Wt.	Molecular Weight
NDM-1	New Delhi Metallo-β-Lactamase-1
PDB	Protein Data Bank
P-gp	P-glycoprotein
RMSD	Root Mean Square Deviation
SD	Standard Deviation
TSA	Tryptic Soy Agar
VDss	Volume of Distribution at Steady State
WHO	World Health Organization

References

1. Murray, C. J.; Ikuta, K. S.; Sharara, F.; Swetschinski, L.; Aguilar, G. R.; Gray, A.; Tasak, N. Global burden of bacterial antimicrobial resistance in 2019: a systematic analysis. *Lancet* **2022**, *399*, 629-655, https://doi.org/10.1016/S0140-6736(21)02724-0.
2. WHO. Antimicrobial Resistance and the United Nations Sustainable Development Cooperation Framework: Guidance for United Nations Country Teams. World Health Organization: **2021**.

3. WHO. Global Antimicrobial Resistance and Use Surveillance System (GLASS) Report: **2022**. World Health Organization: **2022**.
4. Antony, T.; Senthilnathan, Y.; Madhavakumar, R.; Amudhan, P.; Venkataraman, S.; Rally, S.; Pitani, R.S.; Arumugam, I. Comparative evaluation of colistin-susceptibility testing in carbapenem-resistant Klebsiella pneumoniae using VITEK, colistin broth disc elution and colistin broth microdilution. *Cureus* **2024**, *16*, e65796, https://doi.org/10.7759/cureus.65796.
5. Yong, D.; Toleman, M.A.; Giske, C. G.; Cho, H.S.; Sundman, K.; Lee, K.; Walsh, T.R. Characterization of a new metallo-β-lactamase gene, bla NDM-1 and a novel erythromycin esterase gene carried on a unique genetic structure in Klebsiella pneumoniae sequence type 14 from India. Antimicrobial Agents and *Chemotherapy* **2009**, *53*, 5046-5054, https://doi.org/10.1128/AAC.00774-09.
6. Wu, W.; Feng, Y.; Tang, G.; Qiao, F.; McNally, A.; Zong, Z. NDM metallo-β-lactamases and their bacterial producers in health care settings. *Clin. Microbiol. Rev.* **2019**, *32*, e00115-18, https://doi.org/10.1128/CMR.00115-18.
7. Meng, W.; Liu, C.; Wu, G.; Bai, Z.; Wang, Z.; Chen, S.; Wan, S.; Liu, W. Design, synthesis and antibacterial activity evaluation of ebselen derivatives in NDM-1-producing bacteria. *RSC Med. Chem.* **2024**, *15*, 1959-1972, https://doi.org/10.1039/d4md00031e.
8. Lv, H.; Zhu, Z.; Qian, C.; Li, T.; Han, Z.; Zhang, W.; Si, X.; Wang, J.; Deng, X.; Li, L.; Fang, T.; Xia, J.; Wu, S.; Zhou, Y. Discovery of isatin-β-methyldithiocarbazate derivatives as New Delhi metallo-β-lactamase-1 (NDM-1) inhibitors against NDM-1 producing clinical isolates. *Biomed. Pharmacother.* **2023**, *166*, 115439, https://doi.org/10.1016/j.biopha.2023.115439.
9. Yoshizumi, A.; Ishii, Y.; Livermore, D. M.; Woodford, N.; Kimura, S.; Saga, T.; Harada, S.; Yamaguchi, K.; Tateda, K. Efficacies of calcium–EDTA in combination with imipenem in a murine model of sepsis caused by Escherichia coli with NDM-1 β-lactamase. *J. Infect. Chemother.* **2023**, *19*, 992-995, https://doi.org/10.1007/s10156-012-0528-y.
10. Kang, P. W.; Su, J. P.; Sun, L. Y.; Gao, H.; Yang, K. W. 3-Bromopyruvate as a potent covalently reversible inhibitor of New Delhi metallo-β-lactamase-1 (NDM-1). *Eur. J. Pharm. Sci.* **2020**, *142*, 105161, https://doi.org/10.1016/j.ejps.2019.105161.
11. Hecker, S.J.; Reddy, K.R.; Lomovskaya, O.; Griffith, D.C.; Rubio-Aparicio, D.; Nelson, K.; Tsivkovski, R.; Sun, D.; Sabet, M.; Tarazi, Z.; Parkinson, J.; Totrov, M.; Boyer, S.H.; Glinka, T.W.; Pemberton, O.A.; Chen, Y.; Dudley, M.N. Discovery of cyclic boronic acid QPX7728, an ultrabroad-spectrum inhibitor of serine and metallo-β-lactamases. *J. Med. Chem.* **2020**, *63*, 7491-7507, https://doi.org/10.1021/acs.jmedchem.9b01976.
12. Grewal, A.S.; Thapa, K.; Sharma, N.; Singh, S. New Delhi metallo-β-lactamase-1 inhibitors for combating antibiotic drug resistance: recent developments. *Med. Chem. Res.* **2020**, *29*, 1301–1320, https://doi.org/10.1007/s00044-020-02580-x.
13. Sharma, D.; Yadav, J.P. An overview of phytotherapeutic approaches for the treatment of tuberculosis. *Mini Rev. Med. Chem.* **2017**, *17*, 167-183, https://doi.org/10.2174/1389557516666160505114603.
14. 1. Roy, M.; Adhikari, M.; Tiwary, B. Phytocompound-mediated inhibition of quorum-sensing cascade in pathogenic bacteria. In Natural Products, 1st Edition; Roy, M.P., Adhikari, M.D., Tiwary, B.K., Eds.; CRC Press: Boca Raton, **2023**; pp. 79-101, https://doi.org/10.1201/9781003300557-5.
15. Ao, M.; Lhungdim, H. Cultural affinity and preferences for traditional medicine and its providers over modern healthcare services in Nagaland, India. *Demography India* **2020**, *49*, 106-122.
16. Pandey, G.; Madhuri, S. Some medicinal plants as natural anticancer agents. *Pharmacogn. Rev.* **2009**, *3*, 259-263.
17. Kumar, M.P.; Anisha, S.; Dhrisya, C.; Becky, R.; Sadhasivam, S. Therapeutic and pharmacological efficacy of selective Indian medicinal plants–a review. *Phytomed. Plus* **2021**, *1*, 100029, https://doi.org/10.1016/j.phyplu.2021.100029.
18. Asiamah, I.; Obiri, S.A.; Tamekloe, W.; Armah, F.A.; Borquaye, L.S. Applications of molecular docking in natural products-based drug discovery. *Sci. Afr.* **2023**, *20*, e01593, https://doi.org/10.1016/j.sciaf.2023.e01593.
19. Rahman, M.; Khan, M. K.A. In silico based unraveling of New Delhi metallo-β-lactamase (NDM-1) inhibitors from natural compounds: a molecular docking and molecular dynamics simulation study. *J. Biomol. Struct. Dyn.* **2020**, *38*, 2093-2103, https://doi.org/10.1080/07391102.2019.1627248.
20. Salari-jazi, A.; Mahnam, K.; Sadeghi, P.; Damavandi, M. S.; Faghri, J. Discovery of potential inhibitors against New Delhi metallo-β-lactamase-1 from natural compounds: in silico-based methods. *Sci. Rep.*

2021, *11*, 2390, https://doi.org/10.1038/s41598-021-82009-6.
21. Shi, C.; Chen, J.; Xiao, B.; Kang, X.; Lao, X.; Zheng, H. Discovery of NDM-1 inhibitors from natural products. *J. Glob. Antimicrob. Resist.* **2019**, *18*, 80-87, https://doi.org/10.1016/j.jgar.2019.02.003.
22. Pal, A.; Tripathi, A. Quercetin inhibits carbapenemase and efflux pump activities among carbapenem-resistant Gram-negative bacteria. *APMIS* **2020**, *128*, 251-259, https://doi.org/10.1111/apm.13015.
23. Liu, S.; Zhang, J.; Zhou, Y.; Hu, N.; Li, J.; Wang, Y.; Niu, X.; Deng, X.; Wang, J. Pterostilbene restores carbapenem susceptibility in New Delhi metallo-β-lactamase producing isolates by inhibiting the activity of New Delhi metallo-β-lactamases. *Br. J. Pharmacol.* **2019**, *176*, 4548-4557, https://doi.org/10.1111/bph.14818.
24. Sharahi, J.Y.; Ahovan, Z.A.; Maleki, D.T.; Rad, Z.R.; Rad, Z.R.; Goudarzi, M.; Shariati, A.; Bostanghadiri, N.; Abbasi, E.; Hashemi, A. In vitro antibacterial activity of curcumin meropenem combination against extensively drug-resistant (XDR) bacteria isolated from burn wound infections. *Avicenna J. Phytomed.* **2020**, *10*, 3-10.
25. Kar, S.; Leszczynski, J. Open access in silico tools to predict the ADMET profiling of drug candidates. *Expert Opin. Drug Discov.* **2020**, *15*, 1473-1487, https://doi.org/10.1080/17460441.2020.1798926.
26. Rather, L.J.; Islam, S.U.; Mohammad, F. Acacia nilotica (L.): A review of its traditional uses, phytochemistry, and pharmacology. *Sustain. Chem. Pharm.* **2015**, *2*, 12–30, https://doi.org/10.1016/j.scp.2015.08.002.
27. Maldini, M.; Montoro, P.; Hamed, A. I.; Mahalel, U. A.; Oleszek, W.; Piacente, S. Strong antioxidant phenolics from Acacia nilotica: Profiling by ESI-MS and qualitative–quantitative determination by LC-ESI-MS. *J. Pharm. Biomed. Anal.* **2011**, *56*, 228–239, https://doi.org/10.1016/j.jpba.2011.05.019.
28. Alzohairy, M.A. Therapeutics role of Azadirachta indica (Neem) and their active constituents in diseases prevention and treatment. *Evid.-Based Complement. Altern. Med.* **2016**, *2016*, 7382506, https://doi.org/10.1155/2016/7382506.
29. Islas, J.F.; Acosta, E.; G-Buentello, Z.; Delgado-Gallegos, J.L.; Moreno-Treviño, M.G.; Escalante, B.; Moreno-Cuevas, J.E. An overview of Neem (Azadirachta indica) and its potential impact on health. *J. Funct. Foods* **2020**, *74*, 104171, https://doi.org/10.1016/j.jff.2020.104171.
30. Pradhan, D.; Biswasroy, P.; Haldar, J.; Ghosh, G.; Rath, G. A comprehensive review on phytochemistry, molecular pharmacology, clinical and translational attributes of Ocimum sanctum L. *S. Afr. J. Bot.* **2022**, *150*, 342–360, https://doi.org/10.1016/j.sajb.2022.07.037.
31. Saharkhiz, M.J.; Kamyab, A.A.; Kazerani, N. K.; Zomorodian, K. Chemical compositions and antimicrobial activities of Ocimum sanctum L. essential oils. *Jundishapur J. Microbiol.* ***2015***, *8*, e13720, https://doi.org/10.5812/jjm.13720.
32. Sarup, P.; Bala, S.; Kamboj, S. Pharmacology and phytochemistry of oleo-gum resin of Commiphora wightii (Guggulu). *Scientifica* **2015**, *2015*, 138039, https://doi.org/10.1155/2015/138039.
33. Verma, R.K.; Ibrahim, M.; Fursule, A.; Kumar, B.; Singh, S. Metabolomic profiling of Commiphora wightii reveals guggulsterones and other bioactive terpenoids. *S. Afr. J. Bot.* **2022**, *149*, 211–221, https://doi.org/10.1016/j.sajb.2022.05.060.
34. Upadhyay, A.K.; Kumar, K.; Kumar, A.; Mishra, H.S. Tinospora cordifolia (Guduchi): Validation of the Ayurvedic pharmacology through experimental and clinical studies. *Int. J. Ayurveda Res.* **2010**, *1*, 112–121, https://doi.org/10.4103/0974-7788.64405.
35. Gupta, A.; Gupta, P.; Bajpai, G. Tinospora cordifolia (Giloy): An insight into its immunomodulatory, antimicrobial, and therapeutic potential. *Heliyon* **2024**, *10*, e26125, https://doi.org/10.1016/j.heliyon.2024.e26125.
36. Azwanida, N.N. A review on the extraction methods use in medicinal plants, principle, strength and limitation. *Med. Aromat. Plants* **2015**, *4*, 196.
37. Vuong, Q.V.; Hirun, S.; Roach, P.D.; Bowyer, M.C.; Phillips, P.A.; Scarlett, C.J. Effect of extraction conditions on total phenolic compounds and antioxidant activities of Carica papaya leaf aqueous extracts. *J. Herb. Med.* **2013**, *3*, 104-111, https://doi.org/10.1016/j.hermed.2013.04.004.
38. Harborne, J.B. Phytochemical Methods: A Guide to Modern Techniques of Plant Analysis, 3rd Edition; Chapman & Hall: London, **1998**.
39. Zaidan, M.R. S.; Rain, A. N.; Badrul, A.R.; Adlin, A.; Norazah, A.; Zakiah, I. In vitro screening of five local medicinal plants for antibacterial activity using disc diffusion method. *Trop. Biomed.* **2005**, *22*, 165-170.
40. Ahuatzin-Flores, O.E.; Torres, E.; Chavez-Bravo, E. Acinetobacter baumannii, a multidrug-resistant

opportunistic pathogen in new habitats: A Systematic Review. *Microorganisms* **2024**, *12*, 644. https://doi.org/10.3390/microorganisms12040644.

41. Ahmad, I.; Mehmood, Z.; Mohammad, F. Screening of some Indian medicinal plants for their antimicrobial properties. *J. Ethnopharmacol.* **1998**, *62*, 183–193, https://doi.org/10.1016/S0378-8741(98)00055-5.
42. Kim, S.; Chen, J.; Cheng, T.; Gindulyte, A.; He, J.; He, S.; Li, Q.; Shoemaker, B. A.; Thiessen, P. A.; Yu, B.; Zaslavsky, L.; Zhang, J.; Bolton, E. E. PubChem 2025 update. *Nucleic Acids Res.* **2025**, *53*, D1516-D1525, https://doi.org/10.1093/nar/gkae1059.
43. Daina, A.; Michielin, O.; Zoete, V. SwissADME: a free web tool to evaluate pharmacokinetics, drug-likeness and medicinal chemistry friendliness of small molecules. *Sci. Rep.* **2017**, *7*, 42717, https://doi.org/10.1038/srep42717.
44. Yadav, A.; Mohite, S.K. Prediction and optimization of drug metabolism and pharmacokinetics properties including absorption, distribution, metabolism, excretion and the potential for toxicity properties. *Int. J. Sci. Res. Chem.* **2020**, *5*, 47-58.
45. Trott, O.; Olson, A.J. AutoDock Vina: improving the speed and accuracy of docking with a new scoring function, efficient optimization, and multithreading. *J. Comput. Chem.* **2010**, *31*, 455-461, https://doi.org/10.1002/jcc.21334.
46. Berman, H.M.; Battistuz, T.; Bhat, T.N.; Bluhm, W.F.; Bourne, P.E.; Burkhardt, K.; Feng, Z.; Gilliland, G. L.; Iype, L.; Jain, S.; Fagan, P.; Marvin, J.; Padilla, D.; Ravichandran, V.; Schneider, B.; Thanki, N.; Weissig, H.; Westbrook, J. D.; Zardecki, C. The Protein Data Bank. *Acta Crystallogr. D Biol. Crystallogr.* **2002**, *58*, 899-907, https://doi.org/10.1107/s0907444902003451.
47. Morris, G.M.; Huey, R.; Lindstrom, W.; Sanner, M.F.; Belew, R.K.; Goodsell, D.S.; Olson, A.J. AutoDock4 and AutoDockTools4: Automated docking with selective receptor flexibility. *J. Comput. Chem.* **2009**, *30*, 2785-2791, https://doi.org/10.1002/jcc.21256.
48. Miteva, M.A.; Guyon, F.; Tufféry, P. Frog2: Efficient 3D conformation ensemble generator for small compounds. *Nucleic Acids Res.* **2010**, *38*, W622-W627, https://doi.org/10.1093/nar/gkq325.
49. Pires, D.E.V.; Blundell, T.L.; Ascher, D.B. pkCSM: Predicting Small-Molecule Pharmacokinetic and Toxicity Properties Using Graph-Based Signatures. *J. Med. Chem.* **2015**, *58*, 4066-4072, https://doi.org/10.1021/acs.jmedchem.5b00104.
50. Pires, D.E.V.; Kaminskas, L.M.; Ascher, D.B. Prediction and Optimization of Pharmacokinetic and Toxicity Properties of the Ligand. In Computational Drug Discovery and Design, Gore, M., Jagtap, U.B., Eds.; Springer New York: New York, NY, **2018**; Volume 1762, pp. 271-284, https://doi.org/10.1007/978-1-4939-7756-7_14.
51. Veber, D.F.; Johnson, S.R.; Cheng, H.Y.; Smith, B.R.; Ward, K.W.; Kopple, K.D. Molecular properties that influence the oral bioavailability of drug candidates. *J. Med. Chem.* **2002**, *45*, 2615-2623, https://doi.org/10.1021/jm020017n.
52. Lipinski C. A. Rule of five in 2015 and beyond: Target and ligand structural limitations, ligand chemistry structure and drug discovery project decisions. *Adv. Drug Deliv. Rev.* **2016**, *101*, 34-41, https://doi.org/10.1016/j.addr.2016.04.029.
53. Alonso, H.; Bliznyuk, A. A.; Gready, J.E. Combining docking and molecular dynamic simulations in drug design. *Med. Res. Rev.* **2006**, *26*, 531-568, https://doi.org/10.1002/med.20067.
54. Sadybekov, A.V.; Katritch, V. Computational approaches streamlining drug discovery. *Nature* **2023**, *616*, 673-685, https://doi.org/10.1038/s41586-023-05905-z.
55. Banerjee, P.; Eckert, A. O.; Schrey, A. K.; Preissner, R. ProTox-II: A webserver for the prediction of toxicity of chemicals. *Nucleic Acids Res.* **2018**, *46*, W257-W263, https://doi.org/10.1093/nar/gky318.
56. Gleeson, M.P.; Hersey, A.; Montanari, D.; Overington, J. Probing the links between in vitro potency, ADMET and physicochemical parameters. *Nat. Rev. Drug Discov.* **2011**, *10*, 197-208, https://doi.org/10.1038/nrd3367.
57. Madden, J.C.; Enoch, S.J.; Paini, A.; Cronin, M.T.D. A review of in silico tools as alternatives to animal testing: Principles, resources and applications. *ATLA Altern. Lab. Anim.* **2018**, *46*, 443-459, https://doi.org/10.1177/0261192920965977.
58. van de Waterbeemd, H.; Gifford, E. ADMET in silico modelling: Towards prediction paradise? *Nat. Rev. Drug Discov.* **2003**, *2*, 192-204, https://doi.org/10.1038/nrd1032.
59. Jadimurthy, R.; Jagadish, S.; Nayak, S.C.; Kumar, S.; Mohan, C.D.; Rangappa, K.S. Phytochemicals as invaluable sources of potent antimicrobial agents to combat antibiotic resistance. *Life* **2003**, *13*, 948, https://doi.org/10.3390/life13040948.

60. Chandar, B.; Poovitha, S.; Ilango, K.; MohanKumar, R.; Parani, M. Inhibition of New Delhi metallo-β-lactamase 1 (NDM-1) producing Escherichia coli IR-6 by selected plant extracts and their synergistic actions with antibiotics. *Front. Microbiol.* **2017**, *8*, 1580, https://doi.org/10.3389/fmicb.2017.01580.
61. Inbaraj, S.D.; Menezes, G.; Josephine, G.I.; Pan, M.M.; Muthiah, N.S. Antibacterial effect of lantana camara Linn. on gram negative bacteria and NDM-1 strains: an in vitro study. *Asian J. Pharm. Clin. Res.* **2014**, *7*, 11-14.
62. Bai, G.; Pan, Y.; Zhang, Y.; Li, Y.; Wang, J.; Wang, Y.; Teng, W.; Jin, G.; Geng, F.; Cao, J. Research advances of molecular docking and molecular dynamic simulation in recognizing interaction between muscle proteins and exogenous additives. *Food Chem.* **2023**, *429*, 136836, https://doi.org/10.1016/j.foodchem.2023.136836.
63. Vasudevan, A.; Kesavan, D. K.; Wu, L.; Su, Z.; Wang, S.; Ramasamy, M.K.; Hopper, W.; Xu, H. In silico and in vitro screening of natural compounds as broad spectrum β-lactamase inhibitors against Acinetobacter baumannii New Delhi metallo-β-lactamase-1 (NDM-1). *BioMed Res. Int.* **2022**, *2022*, 4230788, https://doi.org/10.1155/2022/4230788.
64. Barman, S.; Phukan, B.; Borah, P. S.; Puzari, M.; Sharma, M.; Chetia, P. An in silico approach to identify potential NDM-1 inhibitors to fight multidrug resistant superbugs. *Curr. Drug Ther.* **2019**, *14*, 79-84, https://doi.org/10.2174/1574885513666180514161513.
65. Chetia, H.; Sharma, D. K.; Sarma, R.; Verma, A. An in silico approach to discover potential inhibitors against multi-drug resistant bacteria producing New-Delhi metallo-β-Lactamase 1 (NDM-1) enzyme. *Int. J. Pharm. Pharm. Sci.* **2014**, *6*, 299-303.
66. Bibi, Z.; Asghar, I.; Ashraf, N. M.; Zeb, I.; Rashid, U.; Hamid, A.; Ali, M. K.; Hatamleh, A. A.; Al-Dosary, M. A.; Ahmad, R.; Ali, M. Prediction of phytochemicals for their potential to inhibit New Delhi Metallo β-Lactamase (NDM-1). *Pharmaceuticals* **2023**, *16*, 1404, https://doi.org/10.3390/ph16101404.
67. Assaf, I.; Al Hakawati, N.; Borjac, J. In-silico study of Lebanese herbal compounds against carbapenem-resistant Acinetobacter baumannii proteins. *Inform. Med. Unlocked* **2023**, *43*, 101409, https://doi.org/10.1016/j.imu.2023.101409.
68. Muhammad, S.A.; Said, M.S.; Rehman, S.U.; Dawood, M.; Qazi, M.A.; Fatima, N. Targeted based drug designing of pimarane diterpenes as potential inhibitors of New Delhi-beta-lactamase. *Pak. J. Zool.* **2018**, *50*, 2135-2140, https://doi.org/10.17582/journal.pjz/2018.50.6.2135.2140.
69. Etminani, F.; Etminani, A.; Hasson, S.O.; Judi, H.K.; Akter, S.; Saki, M. In silico study of inhibition effects of phytocompounds from four medicinal plants against the Staphylococcus aureus β-lactamase. *Inform. Med. Unlocked* **2023**, *37*, 101186, https://doi.org/10.1016/j.imu.2023.101186.
70. Hemlata; Bhat, M. A.; Kumar, V.; Ahmed, M.Z.; Alqahtani, A.S.; Alqahtani, M.S.; Jan, A.T.; Rahman, S.; Tiwari, A. Screening of natural compounds for identification of novel inhibitors against β-lactamase CTX-M-152 reported among Kluyvera georgiana isolates: An in vitro and in silico study. *Microb. Pathog.* **2021**, *150*, 104688, https://doi.org/10.1016/j.micpath.2020.104688.
71. Diaz, A.; Shripushkar, G.; Balaji, S.; Ramakrishnan, J.; Thamotharan, S.; Ramakrishnan, V. Comprehensive screening of marine metabolites against class B1 metallo-β-lactamases of Klebsiella pneumoniae using two pronged in silico approach. *J. Biomol. Struct. Dyn.* **2023**, *41*, 10930-10943, https://doi.org/10.1080/07391102.2022.2159532.
72. Fatima, A.; Javid, A.; Ahmed, M. Exploring beta-lactamase inhibitory potential of common medicinal plants. *J. Microbiol. Mol. Genet.* **2024**, *5*, 21-35, https://doi.org/10.52700/jmmg.v5i1.153.
73. Thakur, P.; Chawla, R.; Goel, R.; Narula, A.; Arora, R.; Sharma, R.K. Augmenting the potency of third-line antibiotics with Berberis aristata: In vitro synergistic activity against carbapenem-resistant Escherichia Coli. *J. Glob. Antimicrob. Resist.* **2016**, *6*, 10-16, https://doi.org/10.1016/j.jgar.2016.01.015.
74. Horie, H.; Chiba, A.; Wada, S. Inhibitory effect of soy saponins on the activity of β-lactamases, including New Delhi metallo-β-lactamase 1. *J. Food Sci. Technol.* **2018**, *55*, 1948-1952, https://doi.org/10.1007/s13197-018-3091-4.
75. Ning, N.Z.; Liu, X.; Chen, F.; Zhou, P.; Hu, L.; Huang, J.; Li, Z.; Huang, J.; Li, T.; Wang, H. Embelin restores carbapenem efficacy against NDM-1-positive pathogens. *Front. Microbiol.* **2018**, *9*, 71, https://doi.org/10.3389/fmicb.2018.00071.
76. Shi, C.; Bao, J.; Sun, Y.; Kang, X.; Lao, X.; Zheng, H. Discovery of Baicalin as NDM-1 inhibitor: Virtual screening, biological evaluation and molecular simulation. *Bioorga. Chem.* **2019**, *88*, 102953, https://doi.org/10.1016/j.bioorg.2019.102953.

Publisher's Note & Disclaimer

Supplementary Materials

Table S1. Phytoconstituents of *A. arabica* (Lam.) Willd.

Code	Phyto-constituents	Structure	Chemical class	Plant part used (extract)	Ref.
A1	3,5-Di-O-methyl-L-arabinose	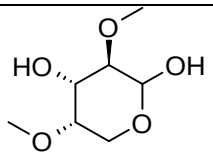	Carbohydrates	Gum	Anderson *et al.*; 1967
A2	2-O-β-L-Arabinofuranosyl-L-arabinose	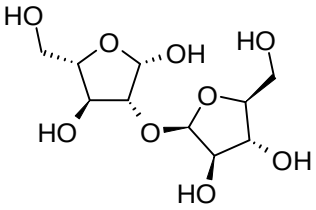	Carbohydrates	Gum	Chalk *et al.*; 1968
A3	Quercetin	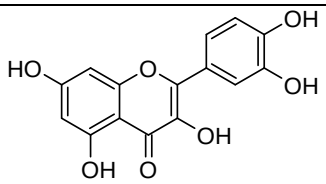	Phenolic compounds	Pods and bark (acetone)	Ayoub, 1984
A4	Catechol	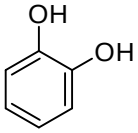	Phenolic compounds	Pods and bark (acetone)	Ayoub, 1984
A5	Gallic acid	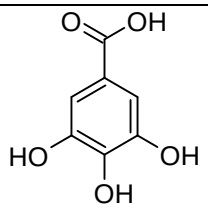	Phenolic compounds	Pods and bark (acetone)	Ayoub, 1984
A6	Catechin	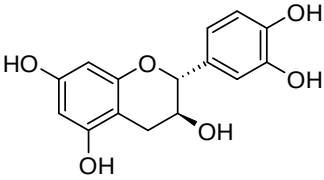	Phenolic compounds	Pods and bark (acetone)	Ayoub, 1984
A7	Epicatechin	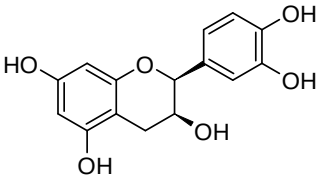	Phenolic compounds	Pods and bark (acetone)	Ayoub, 1984
A8	Epigallocatechin-7-O-gallate	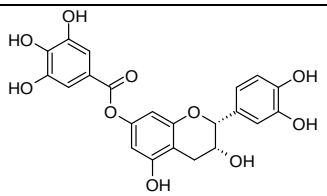	Phenolic compounds	Pods and bark (acetone)	Ayoub, 1984
A9	Epigallocatechin-5,7-O-digallate	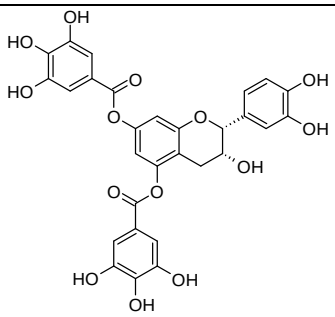	Phenolic compounds	Pods and bark (acetone)	Ayoub, 1984

A10	Palmitic acid	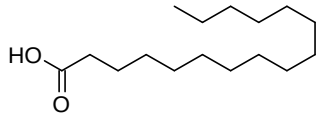	Fatty acids	Seeds (aqueous)	Banerji *et al.*; 1984
A11	Stearic acid	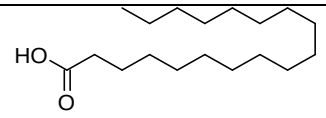	Fatty acids	Seeds (aqueous)	Banerji *et al.*; 1984
A12	Oleic acid	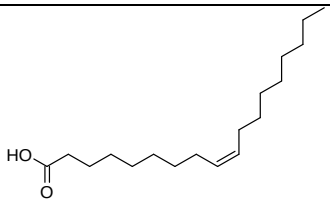	Fatty acids	Seeds (aqueous)	Banerji *et al.*; 1984
A13	Linoleic acid	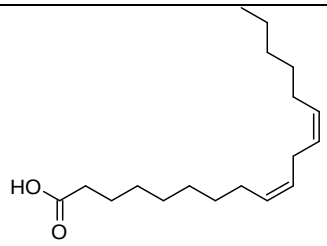	Fatty acids	Seeds (aqueous)	Banerji *et al.*; 1984
A14	Coronaric acid	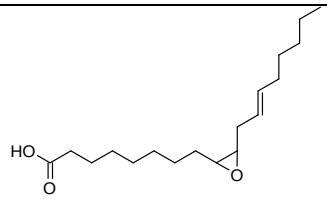	Fatty acids	Seeds (aqueous)	Banerji *et al.*; 1984
A15	Catechin-5-O-gallate	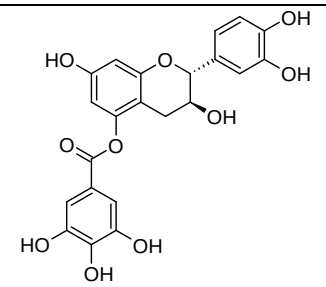	Phenolic compounds	Bark and pods (aqueous methanolic)	Khalid *et al.*; 1989; Salem *et al.*; 2011
A16	Naringenin	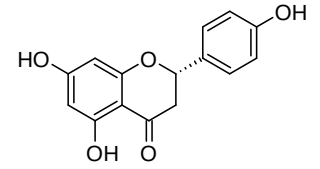	Phenolic compounds	Bark (aqueous methanolic)	Khalid *et al.*; 1989
A17	Catechin-5,7-O-digallate	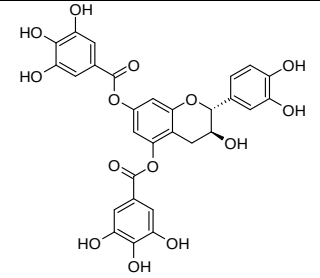	Phenolic compounds	Bark (acetone)	Malan, 1991
A18	Catechin-3′,5-O-digallate	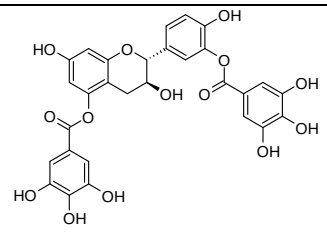	Phenolic compounds	Bark (acetone)	Malan, 1991

A19	Catechin-4′,5-O-digallate	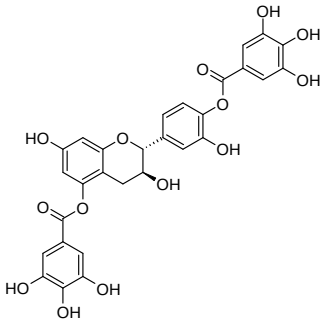	Phenolic compounds	Bark (acetone)	Malan, 1991
A20	D-Galactose	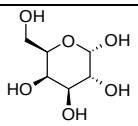	Carbohydrates	Gum	Anderson *et al*.; 1996
A21	L-Arabinose	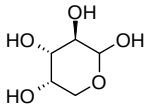	Carbohydrates	Gum	Anderson *et al*.; 1996
A22	L-Rhamnose	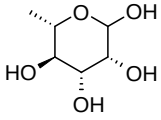	Carbohydrates	Gum	Anderson *et al*.; 1996
A23	6-O-(β-D-Glucopyranosyluronica cid)-D-galactose	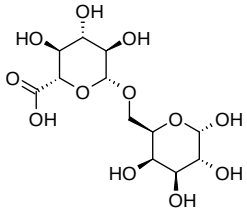	Carbohydrates	Gum	Anderson *et al*.; 1996
A24	6-O-(4-O-Methyl-β-D-glucopyranosyluronica cid)-D-galactose	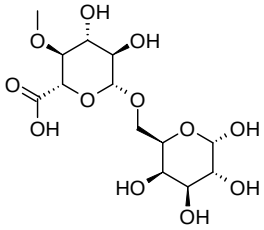	Carbohydrates	Gum	Anderson *et al*.; 1996
A25	4-O-(α-D-Glucopyranosyluronic acid)-D-galactose	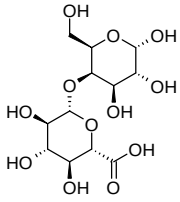	Carbohydrates	Gum	Anderson *et al*.; 1996
A26	4-O-(4-O-Methyl-α-D-glucopyranosyluronica cid)-D-galactose	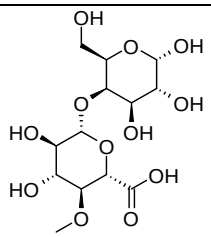	Carbohydrates	Gum	Anderson *et al*.; 1996
A27	Dimethyltryptamine	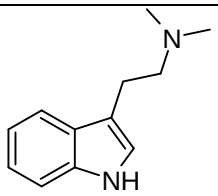	Alkaloids	Leaves (dilute hydrochloric acid)	Camp and Norvell, 1966

A28	5-Methoxy dimethyltryptamine	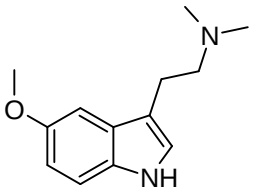	Alkaloids	Leaves (dilute hydrochloric acid)	Camp and Norvell, 1966
A29	N-Methyltryptamine	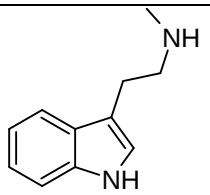	Alkaloids	Leaves (dilute hydrochloric acid)	Camp and Norvell, 1966
A30	3-β-Acetoxy-17-β-hydroxy-androst-5-ene	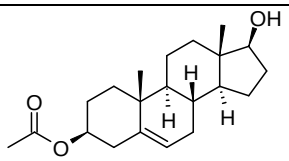	Phytosterols	Aerial parts (methanol)	Chaubal*et al.*; 2003
A31	D-Pinitol	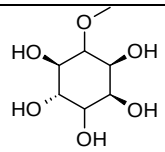	Carbohydrates	Aerial parts (ethanol)	Chaubal *et al.*; 2005
A32	Kaempferol	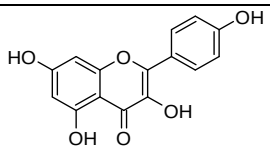	Phenolic compounds	Bark (methanol)	Singh *et al.*; 2008
A33	Protocatechuic acid	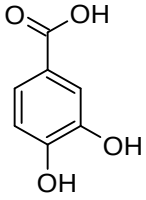	Phenolic compounds	Bark (hexane)	Singh *et al.*; 2009
A34	Caffeic acid	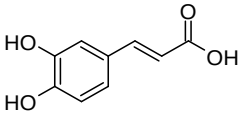	Phenolic compounds	Bark (hexane)	Singh *et al.*; 2009
A35	Ellagic acid	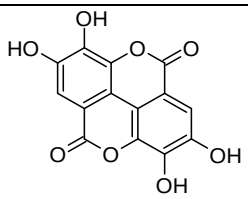	Phenolic compounds	Bark (hexane)	Singh *et al.*; 2009
A36	Rutin (quercetin-3-O-rutinoside)	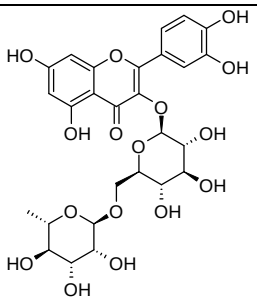	Phenolic compounds	Bark (hexane)	Singh *et al.*; 2009
A37	Apigenin-6,8-bis-C-β-D-glucopyranoside (vicenin)	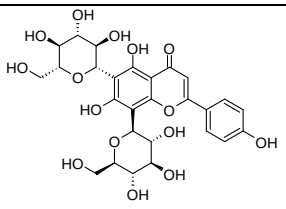	Phenolic compounds	Bark (hexane)	Singh *et al.*; 2009

A38	Naringenin-7-O-β-D-(6′-O-galloyl)glucopyranoside	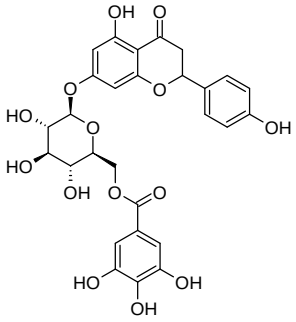	Phenolic compounds	Bark (hexane)	Singh *et al.*; 2009
A39	Kaempferol-7-O-glucoside	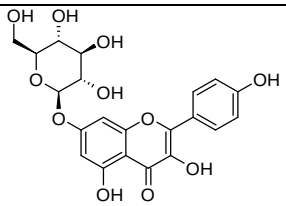	Phenolic compounds	Bark (hexane)	Singh *et al.*; 2009
A40	Acanilol A	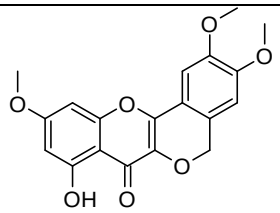	Peltogynoids	Bark (ethanol)	Ahmadu *et al.*; 2010
A41	Acanilol B	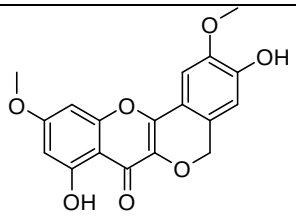	Peltogynoids	Bark (ethanol)	Ahmadu *et al.*; 2010
A42	Lupenone	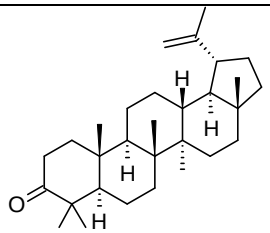	Triterpenes	Bark (ethanol)	Ahmadu *et al.*; 2010
A43	Niloticane	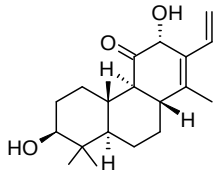	Diterpenes	Bark (ethyl acetate)	Eldeen *et al.*; 2010
A44	1,3-Di-O-galloyl-β-D-glucose	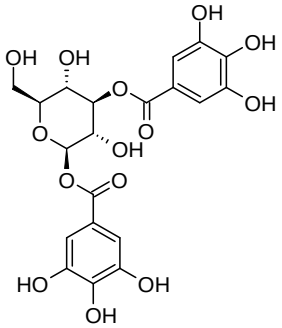	Phenolic compounds	Pods (aqueous ethanolic)	Maldini *et al.*; 2011
A45	1,6-Di-O-galloyl-β-D-glucose	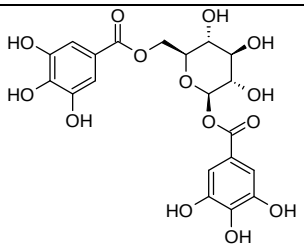	Phenolic compounds	Pods (aqueous ethanolic)	Maldini *et al.*; 2011; Al-Nour *et al.*; 2019

A46	Gallocatechin-7-O-gallate	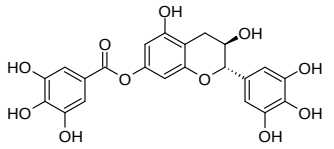	Phenolic compounds	Pods (aqueous ethanolic)	Maldini *et al.*; 2011
A47	Methyl gallate	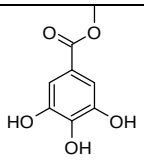	Phenolic compounds	Pods (aqueous ethanolic)	Maldini *et al.*; 2011
A48	Gallocatechin-7,3′-di-O-gallate	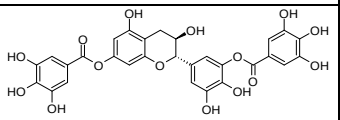	Phenolic compounds	Pods (aqueous ethanolic)	Maldini *et al.*; 2011
A49	Gallocatechin-7,4′-di-O-gallate	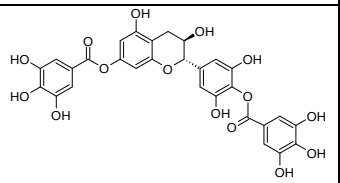	Phenolic compounds	Pods (aqueous ethanolic)	Maldini *et al.*; 2011
A50	Catechin-7-O-gallate	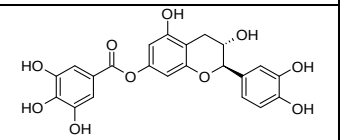	Phenolic compounds	Pods and fruits (aqueous ethanolic)	Maldini *et al.*; 2011
A51	Catechin-7,3′-di-O-gallate	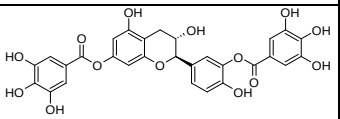	Phenolic compounds	Pods (aqueous ethanolic)	Maldini *et al.*; 2011
A52	Catechin-7,4′-di-O-gallate	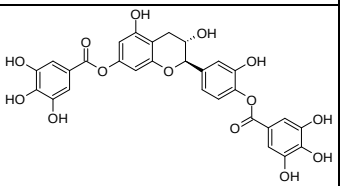	Phenolic compounds	Pods (aqueous ethanolic)	Maldini *et al.*; 2011
A53	Gallocatechin-5-O-gallate	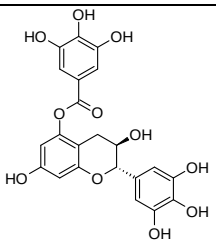	Phenolic compounds	Pods (methanol)	Salem *et al.*; 2011
A54	1-O-Galloyl-β-D-glucose	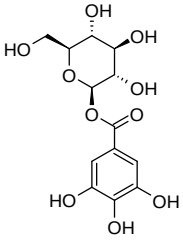	Phenolic compounds	Pods (methanol)	Salem *et al.*; 2011
A55	Digallic acid	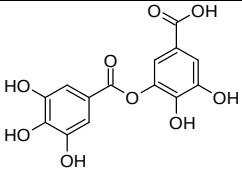	Phenolic compounds	Pods (methanol)	Salem *et al.*; 2011
A56	Ethyl gallate	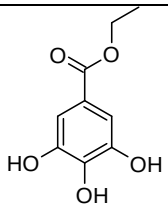	Phenolic compounds	Leaves (ethanol)	Kalaivani *et al.*; 2011

A57	Isoquercetin	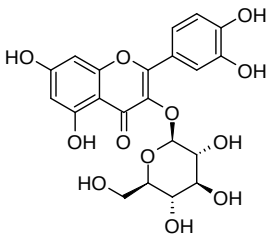	Phenolic compounds	Flowers (methanol)	El-toumy *et al.*; 2011
A58	Naringenin-7-O-β-glucopyranoside	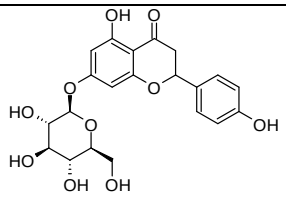	Phenolic compounds	Flowers (methanol)	El-toumy *et al.*; 2011
A59	Chalconaringenin-4′-O-β-glucopyranoside	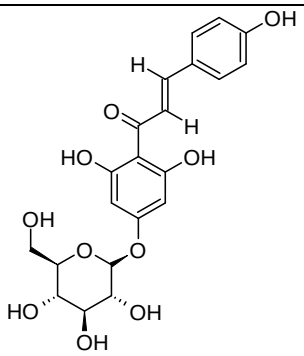	Phenolic compounds	Flowers (methanol)	El-toumy *et al.*; 2011
A60	γ-Sitosterol	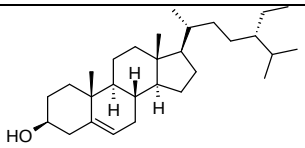	Phytosterols	Leaves (ethanol)	Sundarraj *et al.*; 2012
A61	Flavone	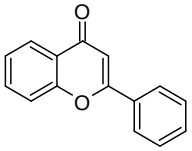	Phenolic compounds	Leaves and bark (methanol)	Bashir *et al.*; 2014
A62	Catechin-3-O-gallate	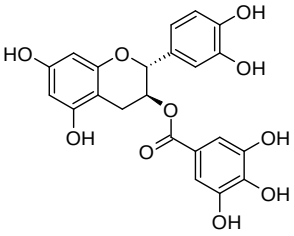	Phenolic compounds	Fruits (hydro-alcoholic)	DiktiVildina *et al.*; 2017
A63	Epicatechin-3-O-gallate	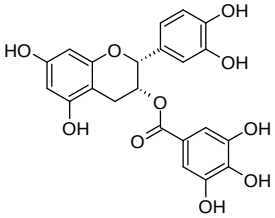	Phenolic compounds	Fruits (hydro-alcoholic)	DiktiVildina *et al.*; 2017
A64	Gallocatechin	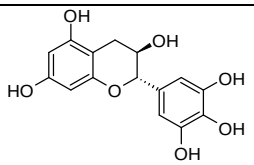	Phenolic compounds	Fruits (hydro-alcoholic)	DiktiVildina *et al.*; 2017
A65	Epigallocatechin	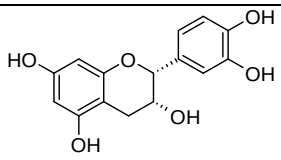	Phenolic compounds	Fruits (hydro-alcoholic)	DiktiVildina *et al.*; 2017

A66	Epigallocatechin-3-O-gallate	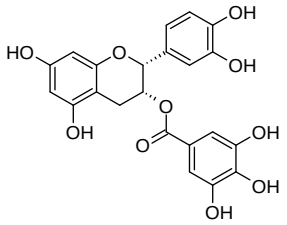	Phenolic compounds	Fruits (hydro-alcoholic)	DiktiVildina *et al*.; 2017
A67	Hexadecane		Hydrocarbons	Seed pods (essential oil using hydro-distillation)	Vivekanandhan *et al*.; 2018
A68	Heptacosan	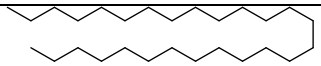	Hydrocarbons	Seed pods (essential oil using hydro-distillation)	Vivekanandhan *et al*.; 2018
A69	Pyrogallol	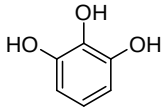	Phenolic compounds	Leaves and fruits (aqueous)	Revathi *et al*.; 2018
A70	Catechin-3,5-O-digallate	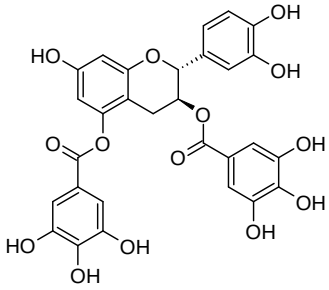	Phenolic compounds	Bark (acetone)	Al-Nour *et al*.; 2019
A71	Mollisacacidin	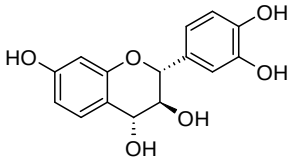	Phenolic compounds	Bark (acetone)	Al-Nour *et al*.; 2019
A72	Acacetin	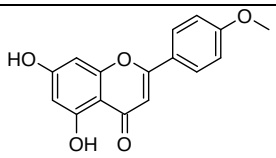	Phenolic compounds	Bark (acetone)	Al-Nour *et al*.; 2019
A73	Chalconaringenin-4-O-β-glucopyranoside	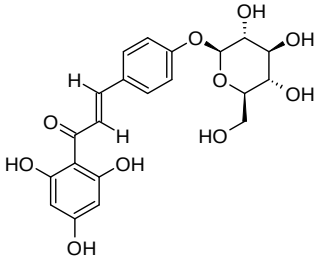	Phenolic compounds	Bark (acetone)	Al-Nour *et al*.; 2019
A74	Leucocyanidin	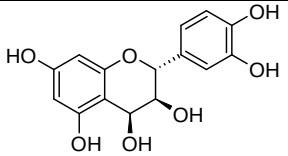	Phenolic compounds	Bark (acetone)	Al-Nour *et al*.; 2019
A75	Lupeol	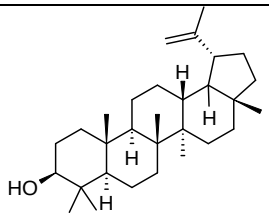	Triterpenes	Bark (acetone)	Al-Nour *et al*.; 2019

A76	Melacacidin	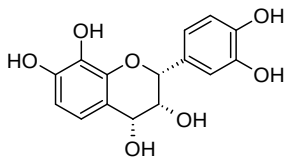	Phenolic compounds	Bark (acetone)	Al-Nour *et al.*; 2019
A77	Nilobamate	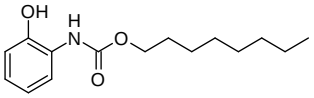	Phenolic compounds	Bark (acetone)	Al-Nour *et al.*; 2019
A78	Apigenin	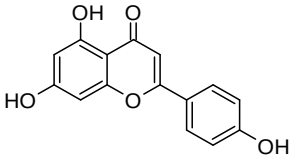	Phenolic compounds	Leaves (aqueous)	SohaibShahzan *et al.*; 2019
A79	Sandynone	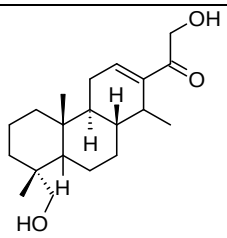	Diterpenes	Root (hexane and ethyl acetate)	Anyam *et al.*; 2021
A80	(5S,7R,8R,9R,10S)-(-)-7,8-seco-7,8-oxacassa-13,15-diene-7,17-diol	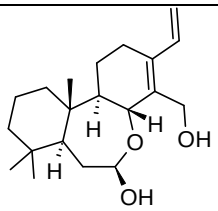	Diterpenes	Root (hexane and ethyl acetate)	Anyam *et al.*; 2021
A81	(5S,7R,8R,9R,10S)-(-)-7,8-seco-7,8-oxacassa-13,15-dien-7-ol-17-al	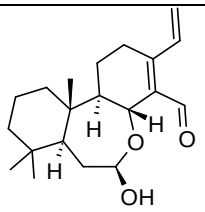	Diterpenes	Root (hexane and ethyl acetate)	Anyam *et al.*; 2021
A82	(5S,7R,8R,9R,10S)-(-)-7,8-seco-7,8-oxacassa-13,15-dien-7-ol	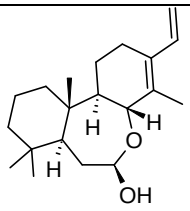	Diterpenes	Root (hexane and ethyl acetate)	Anyam *et al.*; 2021
A83	Stigmasterol	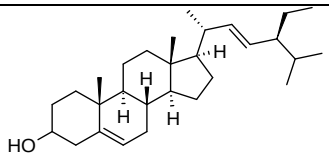	Phytosterols	Root (hexane and ethyl acetate)	Anyam *et al.*; 2021
A84	Chlorogenic acid	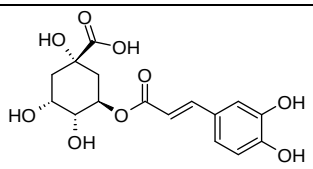	Phenolic compounds	Bark (methanol)	Gautam *et al.*; 2021
A85	Umbelliferone	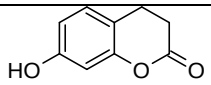	Phenolic compounds	Bark (methanol)	Gautam *et al.*; 2021
A86	N,N-Dimethylglycine	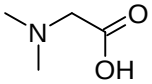	Peptoids	Fruit (methanol)	Rehman *et al.*; 2022
A87	4-Methylbenzenethiol	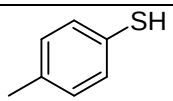	Thiols	Fruit (methanol)	Rehman *et al.*; 2022

A88	(Z,Z)-1,8,11-Heptadecatriene	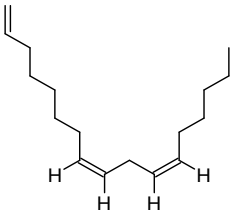	Hydrocarbons	Fruit (methanol)	Rehman *et al.*; 2022
A89	4-O-Methyl mannose	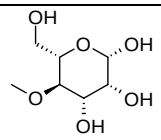	Carbohydrates	Fruit (methanol)	Rehman *et al.*; 2022
A90	Methyl hexadecanoate	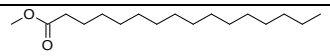	Fatty acid esters	Fruit (methanol)	Rehman *et al.*; 2022
A91	Methyl 14,17-octadecadienoate	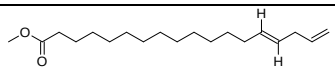	Fatty acid esters	Fruit (methanol)	Rehman *et al.*; 2022
A92	9,12-Octadecadienoic acid	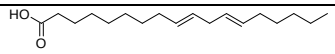	Fatty acids	Fruit (methanol)	Rehman *et al.*; 2022
A93	Methyl oleate	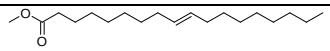	Fatty acid esters	Fruit (methanol)	Rehman *et al.*; 2022
A94	Methyl linoleate	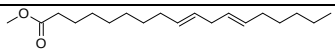	Fatty acid esters	Fruit (methanol)	Rehman *et al.*; 2022
A95	Methyl 9,11-octadecadienoate	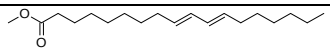	Fatty acid esters	Fruit (methanol)	Rehman *et al.*; 2022
A96	Methyl stearate	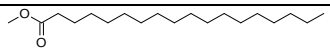	Fatty acid esters	Fruit (methanol)	Rehman *et al.*; 2022
A97	15-Hydroxypentadecanoic acid	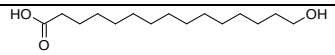	Fatty acids	Fruit (methanol)	Rehman *et al.*; 2022
A98	Glycidyl palmitate	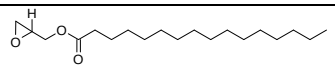	Fatty acid esters	Fruit (methanol)	Rehman *et al.*; 2022
A99	Oxiranylmethyl 9-octadecenoate	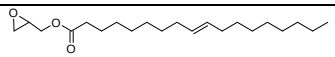	Fatty acid esters	Fruit (methanol)	Rehman *et al.*; 2022
A100	9-Octadecenamide	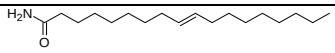	Fatty acids	Fruit (methanol)	Rehman *et al.*; 2022
A101	Bis(2-ethylhexyl) phthalate	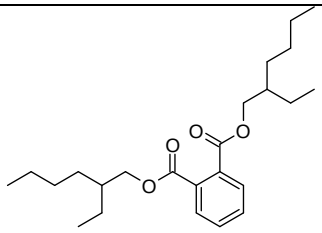	Phthalic acid esters	Fruit (methanol)	Rehman *et al.*; 2022
A102	Ergosta-5,22-dien-3-β-ol	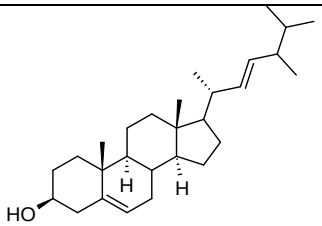	Phytosterols	Fruit (methanol)	Rehman *et al.*; 2022
A103	Ergost-5-en-3-ol	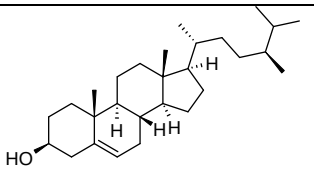	Phytosterols	Fruit (methanol)	Rehman *et al.*; 2022
A104	Betulin	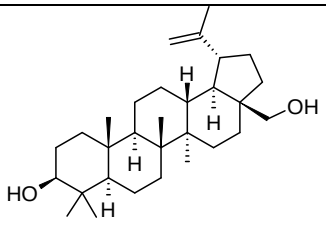	Triterpenes	Bark (chloroform)	Kaur *et al.*; 2022

A105	Clionasterol	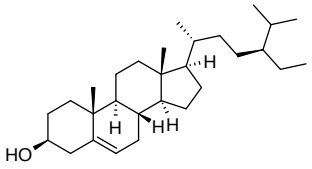	Phytosterols	Bark (ethanol)	Khan *et al.*; 2022
A106	Mangiferin	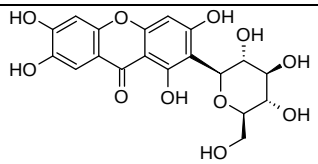	Phenolic compounds	Bark (ethanol)	Khan *et al.*; 2022
A107	α-Copaene	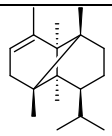	Sesquiterpenes	Bark and fruits (hydro-distilled essential oil)	El Gendy *et al.*; 2022
A108	trans-Caryophyllene	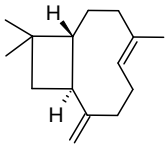	Sesquiterpenes	Bark and fruits (hydro-distilled essential oil)	El Gendy *et al.*; 2022
A109	α-Humulene	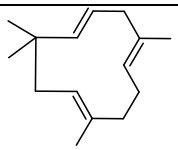	Sesquiterpenes	Bark and fruits (hydro-distilled essential oil)	El Gendy *et al.*; 2022
A110	Germacrene-D	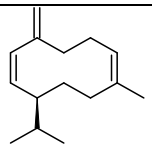	Sesquiterpenes	Bark and fruits (hydro-distilled essential oil)	El Gendy *et al.*; 2022
A111	Myrtenyl acetate	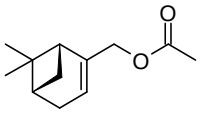	Monoterpenes	Bark (hydro-distilled essential oil)	El Gendy *et al.*; 2022
A112	α-Amorphene	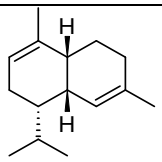	Sesquiterpenes	Bark (hydro-distilled essential oil)	El Gendy *et al.*; 2022
A113	α-Muurolene	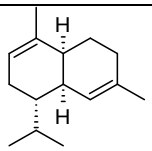	Sesquiterpenes	Bark (hydro-distilled essential oil)	El Gendy *et al.*; 2022
A114	Bicyclogermacrene	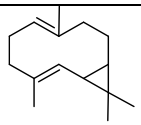	Sesquiterpenes	Bark (hydro-distilled essential oil)	El Gendy *et al.*; 2022
A115	δ-Cadinene	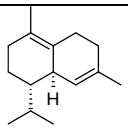	Sesquiterpenes	Bark (hydro-distilled essential oil)	El Gendy *et al.*; 2022
A116	α-Calacorene	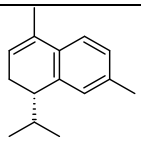	Sesquiterpenes	Bark (hydro-distilled essential oil)	El Gendy *et al.*; 2022
A117	E-Nerolidol	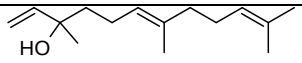	Sesquiterpenes	Bark (hydro-distilled essential oil)	El Gendy *et al.*; 2022

A118	Spathulenol	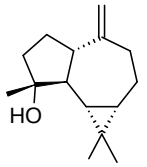	Sesquiterpenes	Bark (hydro-distilled essential oil)	El Gendy *et al.*; 2022
A119	Caryophyllene oxide	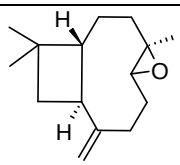	Sesquiterpenes	Bark (hydro-distilled essential oil)	El Gendy *et al.*; 2022
A120	Globulol	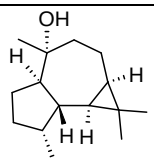	Sesquiterpenes	Bark (hydro-distilled essential oil)	El Gendy *et al.*; 2022
A121	Veridiflorol	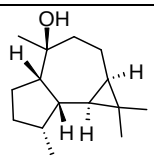	Sesquiterpenes	Bark (hydro-distilled essential oil)	El Gendy *et al.*; 2022
A122	Isospathulenol	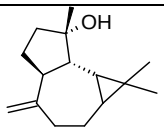	Sesquiterpenes	Bark (hydro-distilled essential oil)	El Gendy *et al.*; 2022
A123	tau-Cadinol	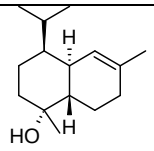	Sesquiterpenes	Bark (hydro-distilled essential oil)	El Gendy *et al.*; 2022
A124	Cubenol	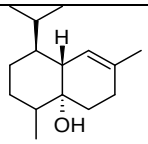	Sesquiterpenes	Bark (hydro-distilled essential oil)	El Gendy *et al.*; 2022
A125	Torreyol	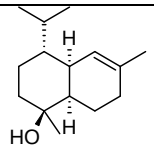	Sesquiterpenes	Bark (hydro-distilled essential oil)	El Gendy *et al.*; 2022
A126	α-Cadinol	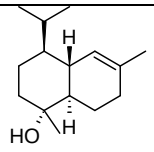	Sesquiterpenes	Bark (hydro-distilled essential oil)	El Gendy *et al.*; 2022
A127	Khusinol	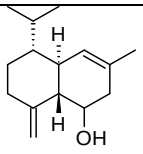	Sesquiterpenes	Bark (hydro-distilled essential oil)	El Gendy *et al.*; 2022
A128	Cryptomeridiol	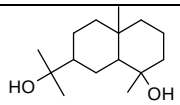	Sesquiterpenes	Bark (hydro-distilled essential oil)	El Gendy *et al.*; 2022
A129	Stachene	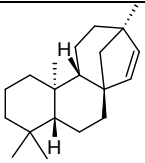	Diterpenes	Bark (hydro-distilled essential oil)	El Gendy *et al.*; 2022
A130	Trachyloban	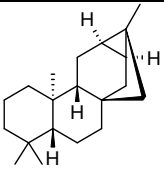	Diterpenes	Bark (hydro-distilled essential oil)	El Gendy *et al.*; 2022

A131	Isokaurene	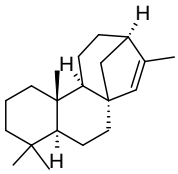	Diterpenes	Bark (hydro-distilled essential oil)	El Gendy *et al.*; 2022
A132	Kaur-16-ene	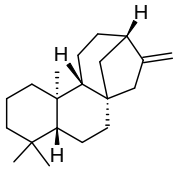	Diterpenes	Bark (hydro-distilled essential oil)	El Gendy *et al.*; 2022
A133	Phytol	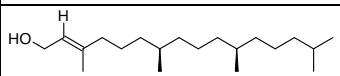	Diterpenes	Bark (hydro-distilled essential oil)	El Gendy *et al.*; 2022
A134	Sclareol	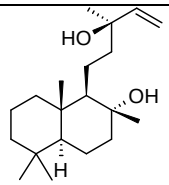	Diterpenes	Bark (hydro-distilled essential oil)	El Gendy *et al.*; 2022
A135	4,8,13-Duvatriene-1,3-diol	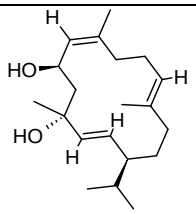	Diterpenes	Bark (hydro-distilled essential oil)	El Gendy *et al.*; 2022
A136	n-Nonacosane	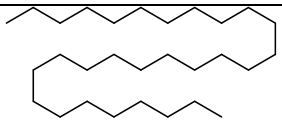	Hydrocarbons	Bark (hydro-distilled essential oil)	El Gendy *et al.*; 2022
A137	n-Dotriacontane	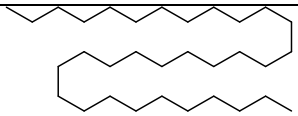	Hydrocarbons	Bark (hydro-distilled essential oil)	El Gendy *et al.*; 2022
A138	α-Pinene	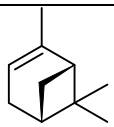	Monoterpenes	Fruits (hydro-distilled essential oil)	El Gendy *et al.*; 2022
A139	β-Pinene	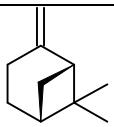	Monoterpenes	Fruits (hydro-distilled essential oil)	El Gendy *et al.*; 2022
A140	1,8-Cineole	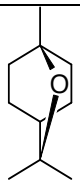	Monoterpenes	Fruits (hydro-distilled essential oil)	El Gendy *et al.*; 2022
A141	γ-Terpinene	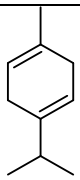	Monoterpenes	Fruits (hydro-distilled essential oil)	El Gendy *et al.*; 2022
A142	α-Linalool	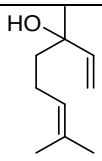	Monoterpenes	Fruits (hydro-distilled essential oil)	El Gendy *et al.*; 2022

A143	Camphor	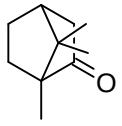	Monoterpenes	Fruits (hydro-distilled essential oil)	El Gendy *et al.*; 2022
A144	Borneol	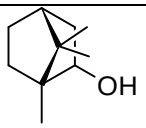	Monoterpenes	Fruits (hydro-distilled essential oil)	El Gendy *et al.*; 2022
A145	4-Terpineol	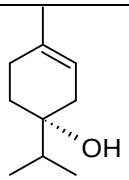	Monoterpenes	Fruits (hydro-distilled essential oil)	El Gendy *et al.*; 2022
A146	α-Terpineol	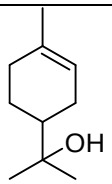	Monoterpenes	Fruits (hydro-distilled essential oil)	El Gendy *et al.*; 2022
A147	Cumin aldehyde	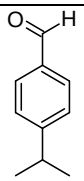	Monoterpenes	Fruits (hydro-distilled essential oil)	El Gendy *et al.*; 2022
A148	Z-Anethole	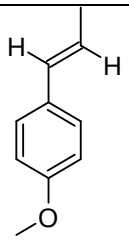	Monoterpenes	Fruits (hydro-distilled essential oil)	El Gendy *et al.*; 2022
A149	Bornyl acetate	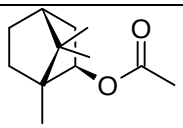	Monoterpenes	Fruits (hydro-distilled essential oil)	El Gendy *et al.*; 2022
A150	2-Caren-10-al	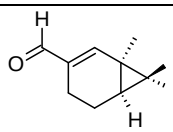	Monoterpenes	Fruits (hydro-distilled essential oil)	El Gendy *et al.*; 2022
A151	α-Terpinyl acetate	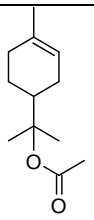	Monoterpenes	Fruits (hydro-distilled essential oil)	El Gendy *et al.*; 2022
A152	α-Elemene	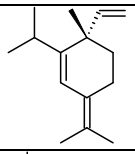	Sesquiterpenes	Fruits (hydro-distilled essential oil)	El Gendy *et al.*; 2022
A153	α-Cubebene	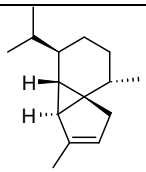	Sesquiterpenes	Fruits (hydro-distilled essential oil)	El Gendy *et al.*; 2022

A154	β-Elemene	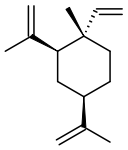	Sesquiterpenes	Fruits (hydro-distilled essential oil)	El Gendy *et al.*; 2022
A155	Methyl eugenol	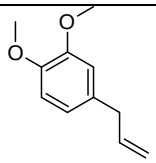	Monoterpenes	Fruits (hydro-distilled essential oil)	El Gendy *et al.*; 2022
A156	Longifolene	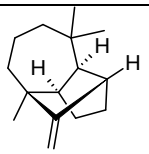	Sesquiterpenes	Fruits (hydro-distilled essential oil)	El Gendy *et al.*; 2022
A157	Aromadendrene	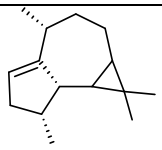	Sesquiterpenes	Fruits (hydro-distilled essential oil)	El Gendy *et al.*; 2022
A158	γ-Muurolene	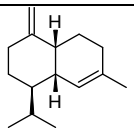	Sesquiterpenes	Fruits (hydro-distilled essential oil)	El Gendy *et al.*; 2022
A159	α-Selinene	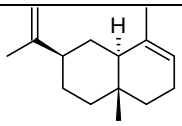	Sesquiterpenes	Fruits (hydro-distilled essential oil)	El Gendy *et al.*; 2022
A160	Tachioside	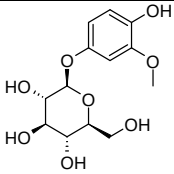	Glycosides	Branch (methanol)	Eiki *et al.*; 2022
A161	(2R,3S)-Piscidic acid	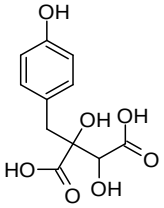	Carboxylic acids	Branch (methanol)	Eiki *et al.*; 2022
A162	1-O-Vanilloyl-β-D-glucose	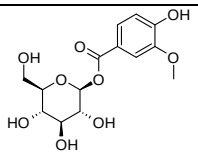	Carbohydrates	Branch (methanol)	Eiki *et al.*; 2022
A163	Methyl isocitric acid	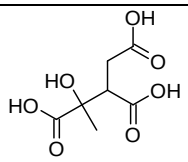	Carboxylic acids	Branch (methanol)	Eiki *et al.*; 2022
A164	3-Methylglutaconic acid	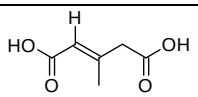	Carboxylic acids	Branch (methanol)	Eiki *et al.*; 2022
A165	L-Tryptophan	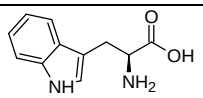	Amino acids	Branch (methanol)	Eiki *et al.*; 2022

Table S2. *In silico* pharmacokinetic prediction of the phytoconstituents of *A. arabica* (Lam.) Willd.

Comp. Code	M.W.	HBAs	HBDs	TPSA	Log $P_{o/w}$ (iLOGP)	Class (solubility)	Lipinski
A1	178.18	5	2	68.15	1.63	Highly soluble	0
A2	178.18	9	6	149.07	0.82	Very soluble	1

A3	178.18	7	5	131.36	1.63	Soluble	0
A4	178.18	2	2	40.46	1.13	Very soluble	0
A5	178.18	5	4	97.99	0.21	Very soluble	0
A6	178.18	6	5	110.38	1.33	Soluble	0
A7	178.18	6	5	110.38	1.47	Soluble	0
A8	178.18	11	8	197.37	1.92	Soluble	2
A9	178.18	14	9	243.9	2.15	Moderately soluble	3
A10	256.42	2	1	37.30	3.85	Moderately soluble	1
A11	284.48	2	1	37.30	4.3	Moderately soluble	1
A12	282.46	2	1	37.30	4.01	Moderately soluble	1
A13	280.45	2	1	37.30	4.01	Moderately soluble	1
A14	296.44	3	1	49.83	3.83	Moderately soluble	0
A15	442.37	10	7	177.14	1.55	Soluble	1
A16	272.25	5	3	86.99	1.75	Soluble	0
A17	594.48	14	9	243.9	2.26	Moderately soluble	3
A18	594.48	14	9	243.9	1.85	Moderately soluble	3
A19	594.48	14	9	243.9	2.38	Moderately soluble	3
A20	180.16	6	5	110.38	0.73	Highly soluble	0
A21	150.13	5	4	90.15	0.59	Highly soluble	0
A22	164.16	5	4	90.15	1.14	Highly soluble	0
A23	356.28	12	8	206.60	-1.48	Highly soluble	2
A24	370.31	12	7	195.60	0.48	Highly soluble	2
A25	356.28	12	8	206.60	-0.76	Highly soluble	2
A26	370.31	12	7	195.60	-1.12	Highly soluble	2
A27	188.27	1	1	19.03	2.21	Soluble	0
A28	290.48	2	0	17.40	3.78	Moderately soluble	0
A29	174.24	1	2	27.82	1.84	Very soluble	0
A30	332.48	3	1	46.53	3.33	Moderately soluble	0
A31	194.18	6	5	110.38	-0.24	Highly soluble	0
A32	286.24	6	4	111.13	1.70	Soluble	0
A33	154.12	4	3	77.76	0.66	Very soluble	0
A34	180.16	4	3	77.76	0.97	Very soluble	0
A35	302.19	8	4	141.34	0.79	Soluble	0
A36	610.52	16	10	269.43	0.46	Soluble	3
A37	594.52	15	11	271.20	1.73	Soluble	3
A38	586.50	14	8	232.90	2.55	Moderately soluble	3
A39	448.38	11	7	190.28	1.55	Soluble	2
A40	356.33	7	1	87.36	3.39	Moderately soluble	0
A41	342.30	7	2	98.36	3.09	Moderately soluble	0
A42	424.70	1	0	17.07	4.54	Poorly soluble	1
A43	318.45	3	2	57.53	2.91	Soluble	0
A44	484.36	14	9	243.9	1.53	Soluble	2
A45	484.36	14	9	243.9	1.43	Soluble	2
A46	458.37	11	8	197.37	1.85	Soluble	2
A47	184.15	5	3	86.99	0.97	Very soluble	0
A48	610.48	15	10	264.13	1.77	Moderately soluble	3
A49	610.48	15	10	264.13	1.86	Moderately soluble	3
A50	442.37	10	7	177.14	2.14	Soluble	1
A51	594.48	14	9	243.90	2.00	Moderately soluble	3
A52	594.48	14	9	243.90	2.40	Moderately soluble	3
A53	458.37	11	8	197.37	1.87	Soluble	2
A54	332.26	10	7	177.14	0.96	Very soluble	1
A55	322.22	9	6	164.75	0.85	Soluble	1
A56	198.17	5	3	86.99	1.21	Soluble	0
A57	464.38	12	8	210.51	0.94	Soluble	2
A58	434.39	10	6	166.14	2.19	Soluble	1
A59	434.39	10	7	177.14	1.53	Soluble	1
A60	414.71	1	1	20.23	5.07	Poorly soluble	1
A61	222.24	2	0	30.21	2.55	Moderately soluble	0
A62	442.37	10	7	177.14	1.59	Soluble	1
A63	442.37	10	7	177.14	1.70	Soluble	1

A64	306.27	7	6	130.61	1.47	Soluble	1
A65	306.27	7	6	130.61	0.98	Soluble	1
A66	442.37	10	7	177.14	1.7	Soluble	1
A67	226.44	0	0	0	4.67	Moderately soluble	1
A68	380.73	0	0	0	7.32	Poorly soluble	1
A69	126.11	3	3	60.69	0.97	Very soluble	0
A70	594.48	14	9	243.90	1.87	Moderately soluble	3
A71	290.27	6	5	110.38	1.35	Soluble	0
A72	284.26	5	2	79.90	2.56	Moderately soluble	0
A73	434.39	10	7	177.14	1.43	Soluble	1
A74	306.27	7	6	130.61	1.19	Very soluble	1
A75	426.72	1	1	20.23	4.72	Poorly soluble	1
A76	306.27	7	6	130.61	1.54	Soluble	1
A77	265.35	3	2	58.56	3.26	Soluble	0
A78	270.24	5	3	90.90	1.89	Soluble	0
A79	320.47	3	2	57.53	2.81	Moderately soluble	0
A80	320.47	3	2	49.69	3.22	Soluble	0
A81	318.45	3	1	46.53	2.69	Moderately soluble	0
A82	304.47	2	1	29.46	3.24	Moderately soluble	1
A83	412.69	1	1	20.23	5.08	Poorly soluble	1
A84	354.31	9	6	164.75	0.87	Very soluble	1
A85	162.14	3	1	50.44	1.44	Soluble	0
A86	103.12	3	1	40.54	1.00	Highly soluble	0
A87	124.20	0	0	38.80	1.99	Soluble	0
A88	234.42	0	0	0	1.99	Soluble	0
A89	194.18	6	4	107.22	-0.10	Highly soluble	0
A90	270.45	2	0	26.30	4.41	Moderately soluble	1
A91	294.47	2	0	26.30	4.54	Moderately soluble	1
A92	280.45	2	1	37.30	4.14	Moderately soluble	1
A93	296.49	2	0	26.30	4.63	Moderately soluble	1
A94	294.47	2	0	26.30	4.63	Moderately soluble	1
A95	294.47	2	0	26.30	4.72	Moderately soluble	1
A96	298.50	2	0	26.30	4.81	Moderately soluble	1
A97	258.40	3	2	57.53	3.31	Soluble	0
A98	312.49	3	0	38.83	4.87	Moderately soluble	0
A99	338.52	3	0	38.83	5.06	Moderately soluble	0
A100	281.48	1	1	43.09	4.22	Moderately soluble	1
A101	390.56	4	0	52.60	4.77	Poorly soluble	1
A102	398.66	1	1	20.23	4.80	Poorly soluble	1
A103	400.68	1	1	20.23	4.83	Poorly soluble	1
A104	442.72	2	2	40.46	4.47	Poorly soluble	1
A105	414.71	1	1	20.23	5.07	Poorly soluble	1
A106	422.34	11	8	201.28	0.89	Soluble	2
A107	246.43	0	0	0	3.59	Moderately soluble	1
A108	204.35	0	0	0	3.25	Soluble	1
A109	204.35	0	0	0	3.27	Soluble	1
A110	204.35	0	0	0	3.31	Moderately soluble	1
A111	194.27	2	0	26.30	2.85	Soluble	0
A112	204.35	0	0	0	3.33	Soluble	1
A113	204.35	0	0	0	3.33	Soluble	1
A114	204.35	0	0	0	3.25	Soluble	1
A115	204.35	0	0	0	3.41	Soluble	1
A116	200.32	0	0	0	3.13	Moderately soluble	1
A117	222.37	1	1	20.23	3.64	Soluble	0
A118	220.35	1	1	20.23	3.04	Soluble	0
A119	220.35	1	0	12.53	3.15	Soluble	0
A120	222.37	1	1	20.23	3.01	Soluble	0
A121	222.37	1	1	20.23	3.11	Soluble	0
A122	220.35	1	1	20.23	3.10	Soluble	0
A123	222.37	1	1	20.23	3.21	Soluble	0
A124	222.37	1	1	20.23	3.24	Soluble	0

A125	222.37	1	1	20.23	3.17	Soluble	0
A126	222.37	1	1	20.23	3.15	Soluble	0
A127	220.35	1	1	20.23	3.14	Soluble	0
A128	240.38	2	2	40.46	2.89	Soluble	0
A129	272.47	0	0	0	0	Poorly soluble	1
A130	272.47	0	0	0	3.74	Moderately soluble	1
A131	272.47	0	0	0	3.78	Moderately soluble	1
A132	272.47	0	0	0	3.74	Moderately soluble	1
A133	296.53	1	1	20.23	4.85	Moderately soluble	1
A134	308.50	2	2	40.46	3.46	Moderately soluble	0
A135	306.48	2	2	40.46	3.51	Moderately soluble	0
A136	408.79	0	0	0	7.79	Insoluble	1
A137	450.87	0	0	0	8.40	Insoluble	1
A138	136.23	0	0	0	2.63	Soluble	1
A139	136.23	0	0	0	2.59	Soluble	1
A140	154.25	1	0	9.23	2.58	Soluble	0
A141	136.23	0	0	0	2.73	Soluble	0
A142	154.25	1	1	20.23	2.70	Soluble	0
A143	152.23	1	0	17.07	2.12	Soluble	0
A144	154.25	1	1	20.23	2.33	Soluble	0
A145	154.25	1	1	20.23	2.51	Soluble	0
A146	154.25	1	1	20.23	2.51	Soluble	0
A147	148.20	1	0	17.07	2.03	Soluble	0
A148	148.20	1	0	9.23	2.51	Soluble	0
A149	196.29	2	0	26.30	2.50	Soluble	0
A150	150.22	1	0	17.07	2.14	Soluble	0
A151	196.29	2	0	26.3	2.93	Soluble	0
A152	204.35	0	0	0	3.46	Moderately soluble	1
A153	204.35	0	0	0	3.40	Soluble	1
A154	204.35	0	0	0	3.37	Moderately soluble	1
A155	178.23	2	0	18.46	2.65	Soluble	0
A156	204.35	0	0	0	3.14	Moderately soluble	1
A157	204.35	0	0	0	3.26	Moderately soluble	1
A158	204.35	0	0	0	3.39	Soluble	1
A159	204.35	0	0	0	3.31	Moderately soluble	1
A160	302.28	8	5	128.84	1.47	Very soluble	0
A161	256.21	7	5	135.29	0.27	Very soluble	0
A162	330.29	9	5	145.91	2.00	Very soluble	0
A163	206.15	7	4	132.13	-0.94	Highly soluble	0
A164	144.13	4	2	74.60	0.64	Very soluble	0
A165	204.23	3	3	79.11	0.99	Very soluble	0

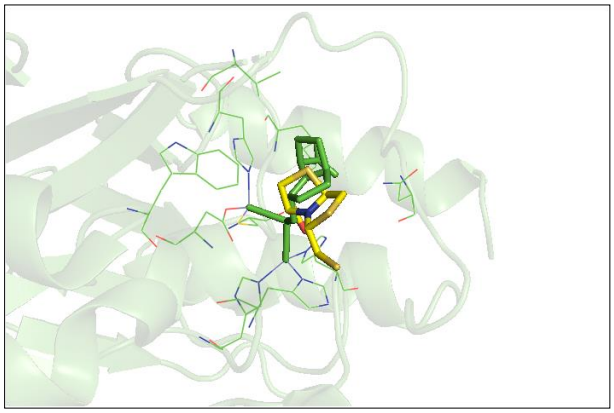

Figure S1. Validation of the docking protocol. The docking protocol was validated via redocking the co-crystallized ligand. The re-docked ligand (yellow) produced a pose similar to that of the co-crystallized ligand (green).